TERMINAL GUIDANCE FOR AUTONOMOUS AERIAL REFUELING

A Thesis

Presented in Partial Fulfillment of the Requirements for

the Degree of Bachelor of Science with Distinction at

The Ohio State University

By

Nicholas S. Higgins

*****

Undergraduate Program in Aeronautical and Astronautical Engineering

The Ohio State University
2011

Undergraduate Examination Committee:

Dr. Clifford A. Whitfield, Advisor

Dr. Gerald M. Gregorek

ABSTRACT

Autonomous Aerial Refueling of Unmanned Aerial Vehicles (UAV-AAR) has been determined to be possible through the development of an autonomous system with terminal guidance capabilities for a probe-and-drogue refueling configuration. An aircraft tanker and UAV were selected for analysis and determination of system constraints. The UAV's mechanics and performance characteristics were determined to understand the aircraft's stability and controllability characteristics. A hardware system necessary for autonomously docking the probe with the drogue was developed using colored light emitting diodes. The flow-field behind an aircraft tanker wing was analyzed to understand the effects of the wake acting on the aircraft to be refueled, and to determine where the pilot must initiate the terminal guidance system. From this analysis, it was determined that the UAV will enter the dangerous flow-field at about 175 feet behind the location of the drogue, approximately 250 feet from the tanker's wing. This area was named the terminal flight arena – the area in which the pilot can no longer control the UAV without a guidance system. Multiple fixed-flight paths for this flight arena were analyzed to determine changing forces acting on the UAV. Utilizing the determined performance characteristics, the control surface deflections necessary for steady flight through these fixed-flight paths were calculated. The best fixed-flight path for UAV-AAR was a path angled ten degrees below a horizontal path, which resulted in

the most minimal change of control surface deflection throughout the terminal flight arena. The overall fixed-flight path control surface deflection analysis will be used to assist in developing a strategy for an autonomous system. The Dual-Optimal Path-Planning technique will be implemented for development of the autonomous system for terminal guidance. The technique will follow a given loop which will allow the UAV to fly within a predetermined window based on the UAV's maneuvering abilities, the locations of minimum induced force that will act on the UAV, the location and orientation of the drogue, and the quickest path for approach and a successful rendezvous.

Dedicated to my family

ACKNOWLEDGMENTS

First and foremost, I share my gratitude for my advisor Dr. Clifford A. Whitfield, for all that he has taught me throughout the course of this research assignment. His dedication of time and efforts encouraged and motivated me to achieve both academically and professionally. Also, thanks to Dr. Gerald M. Gregorek for his guidance and advice as an undergraduate examination committee member.

Sincere thanks needs to be expressed for my colleagues for their aid and encouragement throughout the duration of this study: Jacob Allenstein, Ivan Dusper, Greg Padgett, and Zach Webster.

Finally, I thank Mom, Dad, Candace, Elisa, and Travis. I am extremely grateful for such a wonderful family and their support and encouragement. Without their motivation, this would not have been possible.

VITA

October 7, 1988	Born, Johnstown Ohio, USA
June 12, 2011	B.Sc., Aeronautical and Astronautical Engineering The Ohio State University

FIELDS OF STUDY

Major field: Aeronautical and Astronautical Engineering

TABLE OF CONTENTS

LIST OF FIGURES

LIST OF TABLES

NOMENCLATURE

Parameters

AR	Aspect Ratio	
b	Wing Span	[ft]
C_D	Drag Coefficient	[deg^{-1}]
C_L	Lift Coefficient	[deg^{-1}]
C_l	Rolling Moment Coefficient	[deg^{-1}]
C_m	Pitching Moment Coefficient	[deg^{-1}]
C_n	Yawing Moment Coefficient	[deg^{-1}]
C_y	Side Force Coefficient	[deg^{-1}]
L	Lift	[pounds]
r	Radius	[feet]
S	Wing Area	[ft^2]
V	Velocity	[ft/sec]
W	Weight	[pounds]
α	Angle of Attack	[deg]
β	Sideslip Angle	[deg]
Γ	Circulation	[ft^2/sec]
δA	Aileron Deflection Angle	[deg]
δe	Elevator Deflection Angle	[deg]
δR	Rudder Deflection Angle	[deg]
ρ	Density	[slugs/ft^3]

Abbreviations

AAR	Autonomous Aerial Refueling
CAD	Computer Aided Design
CFD	Computational Fluid Dynamics
LED	Light Emitting Diode
UAV	Unmanned Aerial Vehicle

Subscripts

H	Horizontal Tail
p	Roll Rate
q	Pitch Rate
r	Yaw Rate
V	Vertical Tail
W	Wing
θ	Tangent
0	Origin Location

CHAPTER 1

INTRODUCTION

Unmanned Aerial Vehicles (UAVs) are used to provide services within the U.S. Department of Defense components – services that can sometimes be considered too "dull, dirty, or dangerous" for manned aircraft. The central areas, 'dull' (Intelligence, Surveillance, and Reconnaissance ISR), 'dirty' (atmospheric environment assessment), and 'dangerous' (suppression of enemy air defense) are tasks that UAVs can accomplish within military arenas. The U.S. Military categorizes each UAV based on the vehicle's mission capability and performance characteristics using a tier system. Each military branch has separate parameters within the tier systems, but the concepts for categorization are similar. Micro or small UAVs, such as the RQ-14 Dragon Eye, operate in Tier I, low altitudes from 0 to 25,000 feet. The second tier, Tier II, are vehicles that fly at mid-range altitudes from 25,000 to 50,000 feet and can typically operate for 14 to 28 hours, unrefueled. Examples of Tier II vehicles include the MQ-1 Predator, MQ-9 Reaper, and the ScanEagle. UAVs within the Tier III category operate at altitude at or above 60,000 feet. An example of a Tier III vehicle is the RQ-4 Global Hawk, which has an endurance of 36 hours at an altitude of 65,000 feet.

One constraint that limits UAVs in range is their fuel capacity. For example, requirements are being considered for UAVs to travel overseas instead of being shipped in parts and rebuilt. For Tier II and Tier III UAV operations, using conventional fuel systems causes the vehicle to be limited in range and duration based on its fuel load. Air refueling tankers extend these capabilities for tactical manned military aircraft; however, for unmanned aircraft, UAVs currently lack in-flight capability of docking a refueling probe to the tanker, autonomously. An autonomous system would be advantageous for UAV aerial refueling purposes due to the pilot's location in proximity to the vehicle. For instance, UAVs are typically piloted from a ground control center from up to a few thousand miles from the UAVs actual location. As aircraft approach a refueling tanker, they encounter downwash from the tanker's wing that can cause maneuvering challenges. Being located at a ground control center limits the pilot from sensing the forces acting on the UAV. An autonomous system would take control from the pilot, increasing the potential for successful refueling.

There are two types of common hardware configurations and methods for aerial refueling, boom-and-receptacle and probe-and-drogue. A boom-and-receptacle configuration requires the receiving aircraft to maintain position with respect to the refueling tanker as the refueling boom is extended and steered from the tanker to the vehicle. In a probe-and-drogue configuration, the tanker trails a refueling drogue, an aerodynamically stable basket, and the vehicle to be refueled extends a probe from its nose, wing, or fuel tank, which is flown into the basket. This technique is currently the standard aerial refueling configuration for the U.S. Navy and the air forces of most nations. An advantage to this method is the fact that it does not require a human operator

on-board the tanker, as does the boom-and-receptacle configuration. Also, another advantage of the probe-and-drogue over the boom-and-receptacle is the physical flexibility of the refueling hose and drogue. This physical flexibility allows the drogue to be essentially passive during refueling, allowing the refueling aircraft to move as a response to adverse perturbations in flight such as a gust.

1.1 Objectives

The area behind a tanker requires terminal guidance capability, within the wake effects from the tanker's wing when attaching to the refueling drogue. In order for UAVs to achieve in-flight refueling, the terminal guidance of Autonomous Aerial Refueling (AAR) for UAVs must be developed. Equipping a UAV with the resources for AAR requires terminal guidance technology capable of providing accurate real-time location and orientation measurements of the UAV refueling probe relative to the drogue; and the autonomous capability to successfully dock. UAV-autonomy technologies fall under the following categories[1]:

- *Sensor fusion* – combining information from different sensors for use on-board the vehicle
- *Communications* – handling communications and coordination between multiple agents in the presence of incomplete and imperfect information
- *Path planning* – determining an optimal path for the vehicle to go while meeting certain objectives and mission constraints such as obstacles or fuel requirements

- *Trajectory generation* (sometimes called *Motion planning*) – determining an optimal control maneuver to take to follow a given path or to go from one location to another
- *Trajectory regulation* – the specific control strategies required to constrain a vehicle within some tolerance to a trajectory
- *Task allocation and scheduling* – determining the optimal distribution of tasks amongst a group of agents, with time and equipment constraints
- *Cooperative tactics* – formulating an optimal sequence and spatial distribution of activities between agents in order to maximize chance of success in any given mission scenario

In order for a successful rendezvous, the UAV must have trajectory generation and regulation capability through sensor fusion and task allocation in close proximity to obtain docking with the drogue. A UAV type must first be selected and its mechanics and kinematics defined so that trajectory generation and regulation can be achieved. The area in which the UAV will be flying must also be understood, including flight conditions and atmospheric conditions. This area where the UAV will be flying is determined by the type and size of the tanker aircraft which will generate the wake; therefore, a tanker aircraft must be selected for flow-field analysis. These will provide the limitations for the autonomous system, and must be discussed before UAV-AAR can be developed.

CHAPTER 2

UAV-AAR REQUIREMENTS AND LIMITATIONS

In order to successfully develop an autonomous terminal guidance system for UAV-AAR, constraints and limitations must be defined. Such limitations will determine how and when the system will be initiated. Considered topics include the selection of the aerial refueling method, flight conditions, UAV and refueling tanker type, and hardware/sensor systems.

2.1 Refueling Method

There are two aerial refueling configurations that are commonly used within U.S. Air Force and Navy arenas: boom-and-receptacle (flying boom) and probe-and-drogue refueling techniques. The boom-and-receptacle technique utilizes a boom – a rigid, telescoping tube that an operator on the refueling tanker aircraft extends and inserts into a receptacle on the receiving aircraft. The boom is attached to the rear of the tanker, and can be controlled using flight control surfaces similar to that on an aircraft wing. This technique requires the receiving aircraft to maintain position relative to the tanker and the refueling boom is steered from the tanker to the vehicle. One advantage to the boom-and-receptacle method is that it can refuel at higher fuel-flow rates, enabling a quicker

refueling time. However, smaller aircraft, such as fighters and Tier II UAVs, cannot receive fuel at the boom's maximum flow rate due to their small size and limited abilities to receive high-pressure fuel-flow[2]. Figure 2.1 shows a representation of this boom-and-receptacle refueling method.

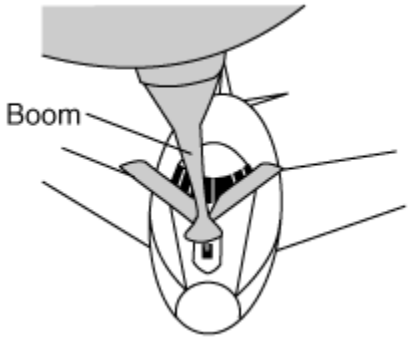

Figure 2.1 – Boom-and-Receptacle Configuration[3]

The probe-and-drogue refueling technique uses a flexible hose which trails from the tanker aircraft's fuel tank and culminates at a drogue. The drogue is a basket which is designed to aerodynamically stabilize the hose while in flight. The receiving vehicle deploys a refueling probe from its nose, wing, or refueling tank, and is flown into the basket. Figure 2.2 displays a diagram of the probe-and-drogue configuration.

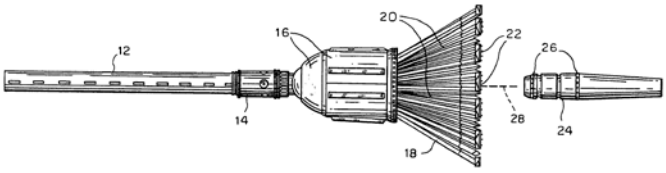

Figure 2.2 – Probe-and-Drogue Configuration[4]

The probe-and-drogue method is the current standard refueling system for the U.S. Navy and the air forces of most nations. This method also does not require a human operator on-board the tanker, as in the case of the boom-and-receptacle configuration. Another advantage of the probe-and-drogue technique over its counterpart is within the physical flexibility of the hose and drogue configuration, essentially passive during refueling, and crucial for small, agile aircraft such as fighters and Tier II UAVs. Fighters and smaller aircraft have the tendency to respond adversely to perturbations while in flight, due to their light weight and/or inherent instabilities. The passivity of the hose allows for small movements of the receiving aircraft, if it were to encounter, for example, a wind gust while refueling.

It is important to select a refueling method for the terminal guidance system; developing one system to utilize both methods would be impractical due to varying flight patterns and aircraft maneuvers to achieve docking in each situation, as well as the use of different hardware configurations. The probe-and-drogue system advantages outweigh the boom-and-receptacle, in two main respects: the physical flexibility of the system for Tier II UAVs and the system is currently the main hardware configuration for the U.S. Navy and air forces of other nations, providing a much broader market of use. Therefore, this refueling approach will be addressed for the support of terminal guidance for UAV-AAR.

2.2 Flight Conditions

The determination of flight conditions for both the refueling tanker and UAV is necessary when considering UAV-AAR. Details such as altitude and airspeed will

provide many parameters for which the system will use. For example, defining an altitude for aerial refueling provides values for ambient pressure, density, and temperature; and with the airspeed, these values will also help determine lift, drag, and other dynamic performance parameters of both aircraft. This information must be known in order to develop an autonomous control system. For aerial refueling, it is important that the tanker aircraft be traveling at a speed in which the UAV can reach its target; in other words, the UAV must be traveling faster than the tanker. The average cruising speed, at altitude, of Tier II UAVs is from 150-200 nautical miles per hour (knots). This limits the tanker aircraft to travel at less than 150 knots; therefore, it was determined that the tanker fly at 130 knots to meet this requirement. Also, to help meet this requirement further, it was determined to fly at an altitude of 20,000 feet for aerial refueling. The average tanker's service ceiling, carrying a full payload, is about 23,000 feet. Flying at 20,000 feet will meet this limitation and provide the conditions necessary for a successful refueling rendezvous. Atmospheric characteristics relevant to this study can be found in Table 2.1.

Table 2.1 – Atmospheric Characteristics at 20,000 feet

Pressure (lb/ft^2)	973.27
Temperature (°R)	447.43
Density ($slugs/ft^3$)	0.001267
UAV Velocity (knots)	150
Tanker Velocity (knots)	130

2.3 UAV and Tanker Selection

As described above, the flight conditions were selected for meeting the limitations of Tier II UAVs and typical tanker aircraft. In order to help define these constraints and

limitations further, specific aircraft must be selected. Refueling tanker aircraft typically used in the U.S. Air Force and Navy consist of aircraft similar to the KC-10, the KC-135, and the C-130. To develop UAV-AAR, a representative aircraft similar to the characteristics of a C-130 will be used. An image of the C-130 is provided in Figure 2.3, along with a list of representative performance characteristics in Table 2.2.

Figure 2.3 – C-130 Hercules[5]

Table 2.2 – Representative Tanker Geometric and Performance Parameters*

W (lb)	135,000
S (ft^2)	1,745
b (ft)	132.6
AR	10.08
V_{AAR} (ft/s)	219.7
$C_{L\text{-}AAR}$	2.512

*values based on C-130

The above table gives tanker parameters for UAV-AAR, where *W* is the weight of the tanker, *S* is the wing area, *b* is the wing span, *AR* denotes the tanker's aspect ratio,

V_{AAR} is the aircraft's velocity for UAV-AAR, and $C_{L\text{-}AAR}$ is the aircraft's lift coefficient for UAV-AAR.

UAV selection involves determining what type of UAV is most popular for present engagements, and will be used most likely in the future; developing a terminal guidance system for UAV-AAR for these types of UAVs should provide a much broader market of use. Presently, UAVs similar to this description exist within the Tier II classification, including the MQ-9 Reaper shown in Figure 2.4. In order to develop terminal guidance, a representative aircraft vehicle will be used, as described in the following subsection.

Figure 2.4 – MQ-9 Reaper[6]

2.3.1 UAV Mechanics

In order to develop the basic control laws necessary for successful UAV-AAR, the kinematics and performance characteristics of the UAV to be used must be determined. As aforementioned, these characteristics were developed utilizing the MQ-9 as a baseline, aiding in the development of a representative UAV. Geometric

considerations, as well as data found in an online U.S. Air Force factsheet, helped to determine performance parameters. Tables 2.3 and 2.4 list some selected geometric and performance characteristics for the representative aircraft.

Table 2.3 – Representative UAV Geometric and Performance Characteristics*

W (lb)	10,500
S_W (ft^2)	257.4
S_H (ft^2)	67.4
S_V (ft^2)	15.7
b (ft)	66
$\bar{c}$ (ft)	3.9
AR	16.9
V_{AAR} (ft/s)	338
$C_{L\text{-}AAR}$	0.5653
$C_{D\text{-}AAR}$	0.0256

*values based on MQ-9 Reaper

Table 2.4 – Representative UAV Stability and Controllability Derivatives*

Longitudinal

$C_{L\alpha}$	$C_{D\alpha}$	$C_{m\alpha}$	C_{lq}	C_{mq}	$C_{m\delta e}$
0.0602	0.0976	-0.0301	0.1267	-0.1459	-0.0058

Lateral/Directional

$C_{y\beta}$	$C_{l\beta}$	$C_{n\beta}$	C_{lp}	C_{np}	C_{lr}	C_{nr}	$C_{l\delta A}$	$C_{n\delta R}$
-0.0071	-3.16e-4	7.67e-4	-0.0051	-0.0013	0.0037	-0.1875	0.0015	-6.09e-4

*All derivatives are per degree, determined based on MQ-9 geometric characteristics

2.4 Hardware Systems

There are multiple methods for how an autonomous system can determine its next set of tasks; in the case of UAV-AAR, path trajectory generation will be determined through sensor fusion. The system must be able to sense where its target is, in order to dock the refueling probe to the drogue. Types of communication between the drogue and the UAV could potentially include light emitters and sensors, laser painting, high

frequency sound transmission, and radio communications. Considering the system will be active while in flight, sound transmission will not be advantageous due to high noise levels created by nearby engines and airflow. Laser painting would require the system to "search" for the drogue without first "knowing" its location, using a tracking system.

Light Emitting Diodes (LEDs) are the most advantageous sensory hardware; the light emitted travels in a radial configuration, allowing the UAV's sensors to pick up the signal from virtually anywhere. This immediately allows the system to point the UAV in the direction of the light, enabling the terminal guidance to quickly generate the optimum path for docking. The emitted lights also allow for the UAV to experience perturbations while flying and maintaining the location of the drogue. These perturbations will be inevitably experienced due to the larger tanker's wing creating instabilities in the airflow and will be discussed further in the following chapter. Work has been done concerning vision-based sensors and navigation systems. For example, a visual system of LEDs placed around a drogue can be used to help the UAV determine the drogue's orientation[7,8]. As an application of this, the LEDs could be colored similarly to an aircraft's wing-tip LEDs for determining orientation. For commercial aircraft, the left wing tip is lit with a red light and the right with a green light. This helps other aircraft determine the direction in which the aircraft is traveling. Likewise, using colored LEDs on the drogue would help the UAV determine the direction of the drogue and how it should attach its probe. Figure 2.5 gives a representation of this system schematic, where the red light represents the left side of the drogue, the green light represents the right side, and the white light provides a third source for orientation determination.

Figure 2.5 – Drogue LED System[9]

With this LED system on the drogue, the UAV should be equipped with a sensor unit capable of reading and tracking colored lights. This method of sensor fusion seems to be the most advantageous for UAV-AAR, and is a proven method as a navigation system.

2.5 Terminal Guidance System Transition

For terminal guidance, "terminal" was coined as a term meaning in which the pilot can no longer control the UAV without the aid of an automatic controller-based system. The UAV must be "guided" through this terminal region, or the area in which the wake of the tanker wing will affect the flight of the UAV during refueling. The autonomous system being developed for UAV-AAR is meant for the UAV's pilot to refrain from controlling the aircraft while the system guides the UAV through the terminal area. This system, which will use the hardware defined previously, is expected to be initiated as the UAV enters this terminal area. This position of transition from piloted flight to autonomous flight will be determined by the range of the LED sensor

equipped by the UAV. The terminal area definition is discussed further in the following chapter, first dealing with aerodynamic effects due to the tanker's wake, and second dealing with the UAV's ground controllers.

CHAPTER 3

UAV-AAR TERMINAL FLIGHT ARENA

The terminal flight arena for UAV-AAR is defined to be the area in which the pilot will initiate the terminal guidance system, which is shown in Figure 3.1. This arena is considered to be too dangerous for a ground-control pilot to fly, due to the wake effects of the tanker aircraft's wing and the finesse required to fly while dynamically tracking and targeting the drogue. For tactical manned aircraft, the process of joining a probe to a drogue in flight is governed by the pilot's ability to adapt and adjust to the turbulent flight conditions. On the other hand, a ground-control pilot for a UAV would not be exposed to this situation. Therefore, a flight arena must be determined in which the terminal guidance system for UAV-AAR can take command.

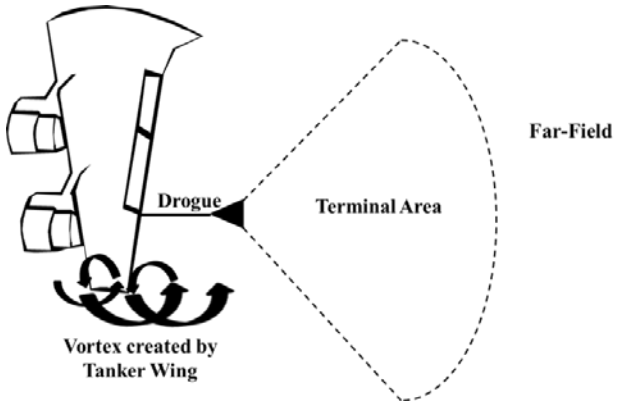

Figure 3.1 – Terminal Area Diagram

3.1 Aerodynamics

Following the condition that, for UAV-AAR, the tanker would be traveling at a speed of 130 knots at an altitude of 20,000 feet, a fluid analysis of the flow-field behind the tanker wing could be achieved. An integration of vortex and circulation theory, as well as computational fluid analysis, was completed. As displayed in Figure 3.1, the tanker wing will create a vortex at the tip of the wing. Typically, the wake from a wing and wing-tip will culminate into a large vortex approximately three-quarters of the half-span of the tanker aircraft. This vortex will develop forces in the flow-field that will act upon the UAV as it attempts aerial refueling. Determining the strength of this merged vortex is a key factor in defining the terminal arena in which terminal guidance for UAV-AAR will occur. In order to understand the behavior of these forces, an integration of vortex and circulation theory as well as computational fluid analysis was completed to develop a velocity profile of the flow-field.

A surface model of a wing representative of the C-130 was designed using Computer Aided Design (CAD) software. The same geometric characteristics found in Table 2.1 were used for the design. An image of this model is shown in Figure 3.2.

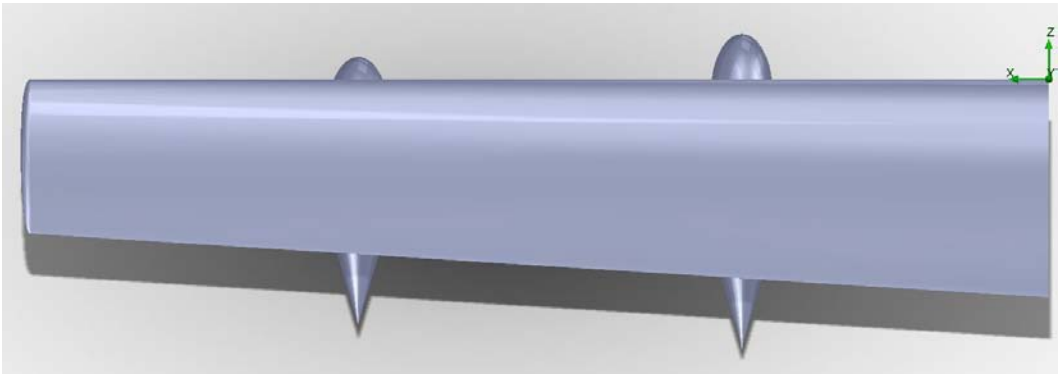

Figure 3.2 – Representative CAD Wing Model

This model was used for completing computational fluid analysis of the wing. This model was imported into a Computational Fluid Dynamics (CFD) software package – FLUENT – with which the fluid analysis could take place. Once the model was imported, flight at altitude was simulated. Conditions were fixed to be at 20,000 feet, characteristics of which can be found in Table 2.1. The flow velocity was set to be the speed at which the tanker will fly for UAV-AAR: 130 knots. After running the simulation and converging on a solution, the following figures demonstrate the velocity profile of the flow-field behind the tanker's wing. Figure 3.3 shows an image of pressure distribution at the drogue's location (marked), while Figure 3.4 shows the more relevant velocity profile for the airspace in consideration.

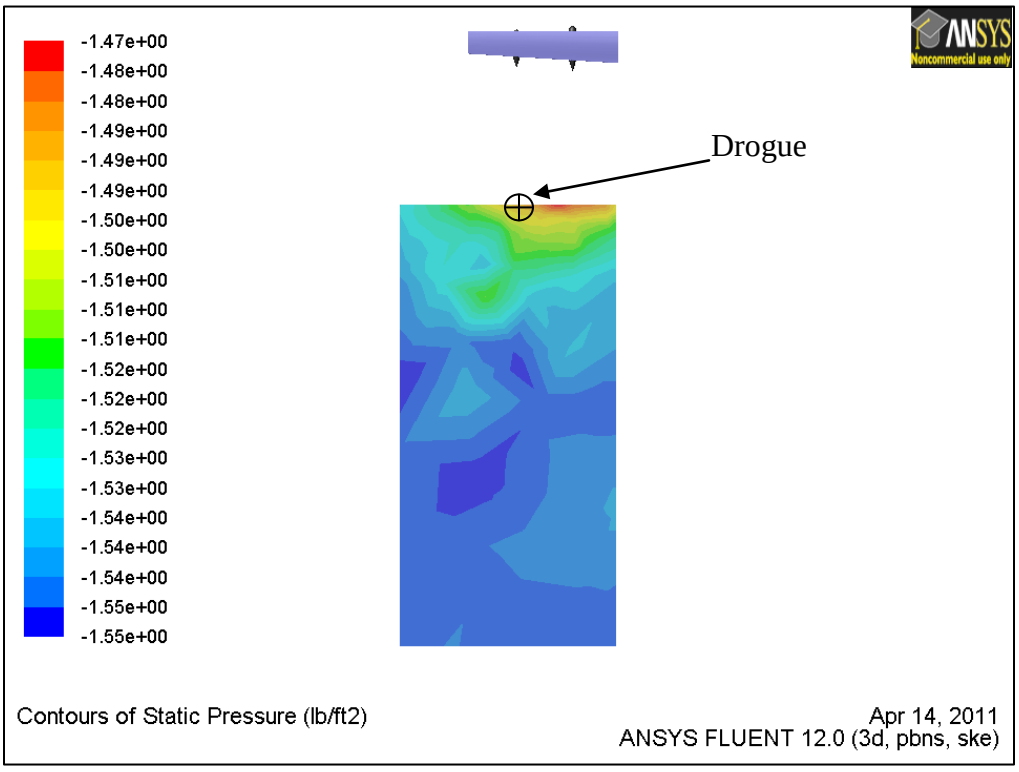

Figure 3.3 – Contours of Static Pressure of Flow-Field

Figure 3.3 shows the static pressure contours for a flow-field starting at the location of the drogue. For this analysis, the drogue was located 45 feet from the wing root, 16 feet below the wing, and 75 feet behind the wing. This position is where a drogue may extend to after deployment. It is assumed here that the drogue will remain static for the duration of terminal guidance. For a real-world case, the drogue will oscillate slightly with the wake produced by the tanker.

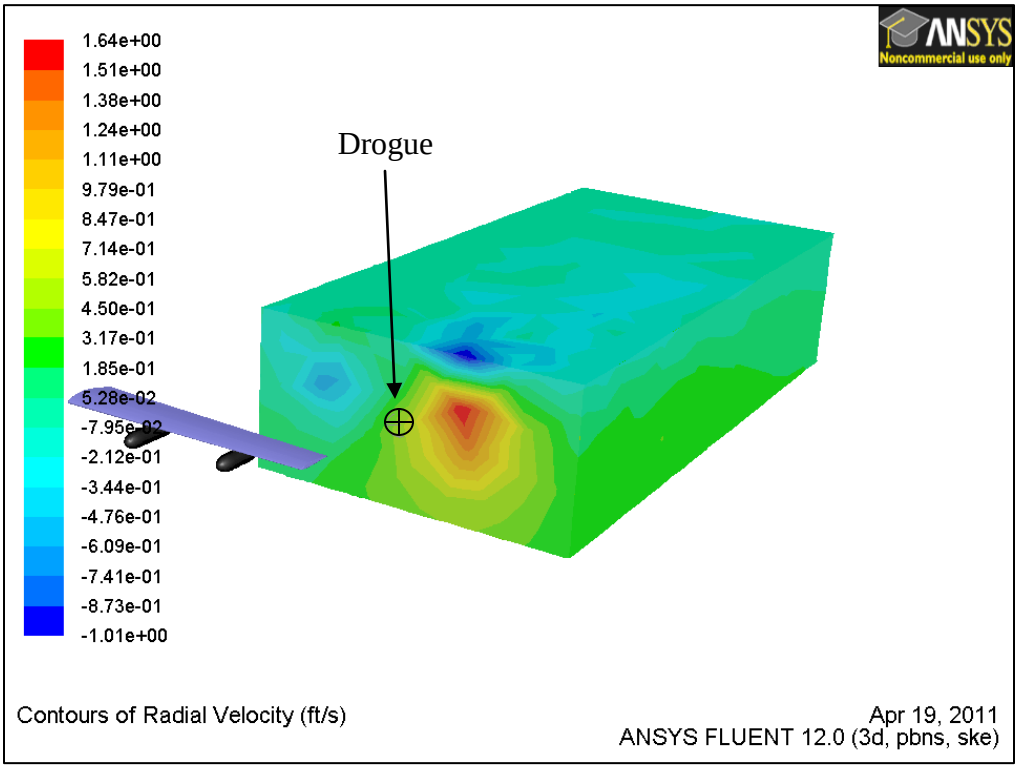

Figure 3.4 – Contours of Radial Velocity

The flow-field shown in Figure 3.4 is 97.5 feet (25 UAV chord lengths) wide by 292.5 feet (75 UAV chord lengths) long. It is important to scale the domain with reference to the UAV to help determine the UAVs location while traveling. There were multiple preliminary computational tests for smaller domain sizes that led to the

determination of this larger flow-field domain. This domain was determined for computational analysis so that it would be large enough to acquire the full "picture" of the wake and vorticity effects in the flow-field and begin the process narrowing this area to define the terminal flight arena. Figure 3.4 also allows for visualization of the vortex being generated by the tanker wing. It can also be seen in this figure that the drogue is located away from the center of the vortex. As will be seen in Chapter 4, it is important to stay clear of the vortex center because aircraft control becomes very difficult.

Along with FLUENT results, fundamental approaches to vortex flows using inviscid, incompressible flow theory were investigated and adapted to the CFD results. The following method from Anderson[10] was applied to the UAV-AAR study. Circulation is defined by Anderson as

$$\Gamma_0 = \frac{L}{\rho V b}$$

where Γ_0 is circulation at the origin (shown in Figure 3.5), L is the lift (weight) of the aircraft, ρ is the density at altitude (Table 2.1), and V and b are defined in Table 2.2.

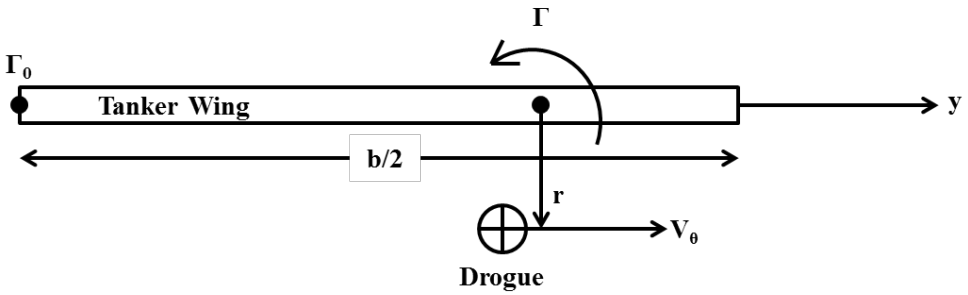

Figure 3.5 – Circulation Schematic

Knowing Γ_0, elliptical lift distribution theory can now be applied to determine the circulation at the vortex location – three-quarters of the tanker's half-span, or the location

of Γ in Figure 3.5. This value for circulation, Γ, was determined using the following relationship:

$$\Gamma(y) = \Gamma_0 \sqrt{1 - \left(\frac{2y}{b}\right)^2}$$

where y is the vortex location. In this case, $y = \left(\frac{3}{4}\right)\left(\frac{b}{2}\right)$, or three-quarters of half-span. In the case of circulation, velocities in the lateral and vertical direction are equivalent to the tangential velocity of the circulating air. This tangential velocity (V_θ) was found using the following equation:

$$V_\theta = \frac{\Gamma}{2\pi r}$$

where r is the vertical distance from the wing to the drogue; previously defined as 16 feet. This method for finding the tangential velocity was then used along with the data as computed by FLUENT CFD. This allowed for the graphical representation of the velocity profile and flow-field behind the tanker's wing, displayed in Figure 3.6; V_x, V_y, V_z correspond to the velocity component in the x-direction, y-direction, and z-direction, respectively, assuming a three-dimensional coordinate system. The plot is for a UAV flight pattern heading straight-on to the drogue, showing the changes in velocity with respect to location in the x-direction.

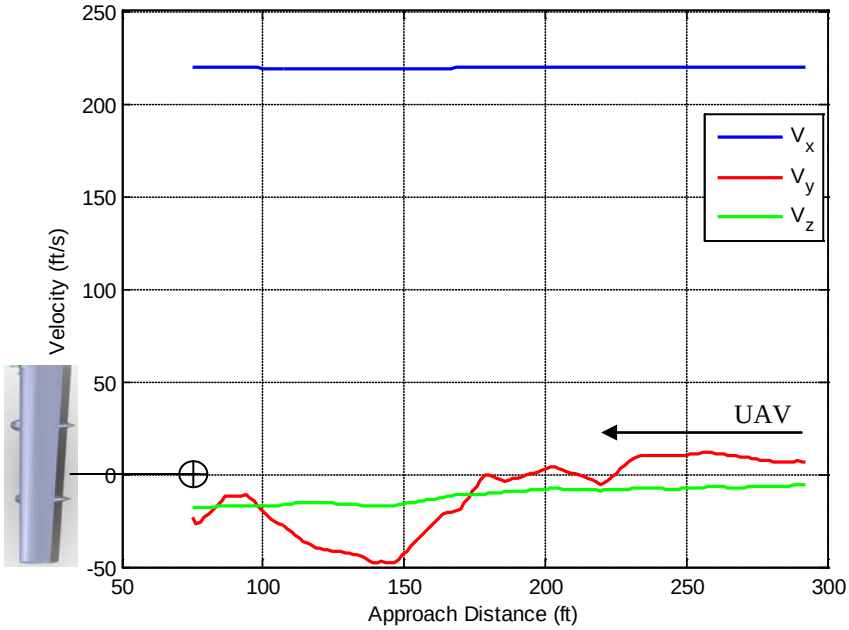

Figure 3.6 – Velocity Profile for Straight-On Approach

According to this graphical representation of velocity, based off of the analysis conducted using FLUENT CFD, the velocity component in the y-direction will be the driving force in developing the control laws necessary for terminal guidance of UAV-AAR. This plot provides insight to where the definition of the terminal arena will start, noting that the most drastic change in V_y occurs at about 230 feet from the wing. Figures 3.7 and 3.8 are a continuation of the CFD analysis, with Figure 3.8 showing a plot of variation of vorticity with distance from the wing.

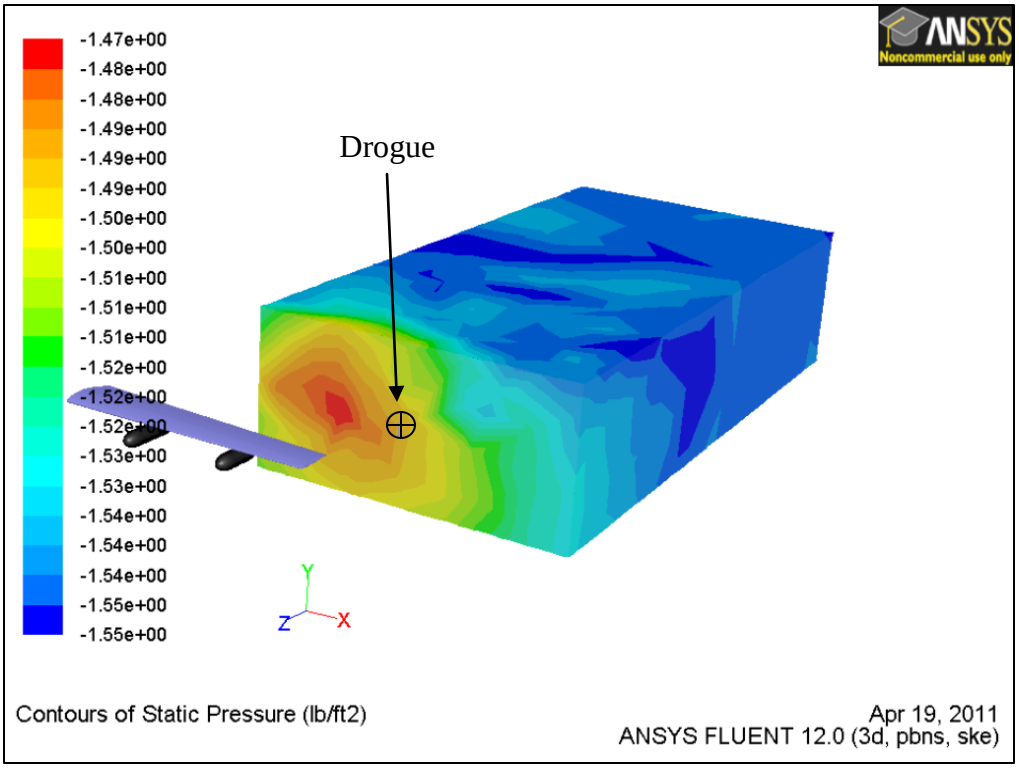

Figure 3.7 – Contours of Static Pressure

The pressure contours shown in Figure 3.7 help to identify where the areas of high and low pressure are occurring. With the plot in Figure 3.8, the vortex can begin to be visualized, and the terminal area even more defined. Section 3.3 will discuss the determined terminal flight arena definition.

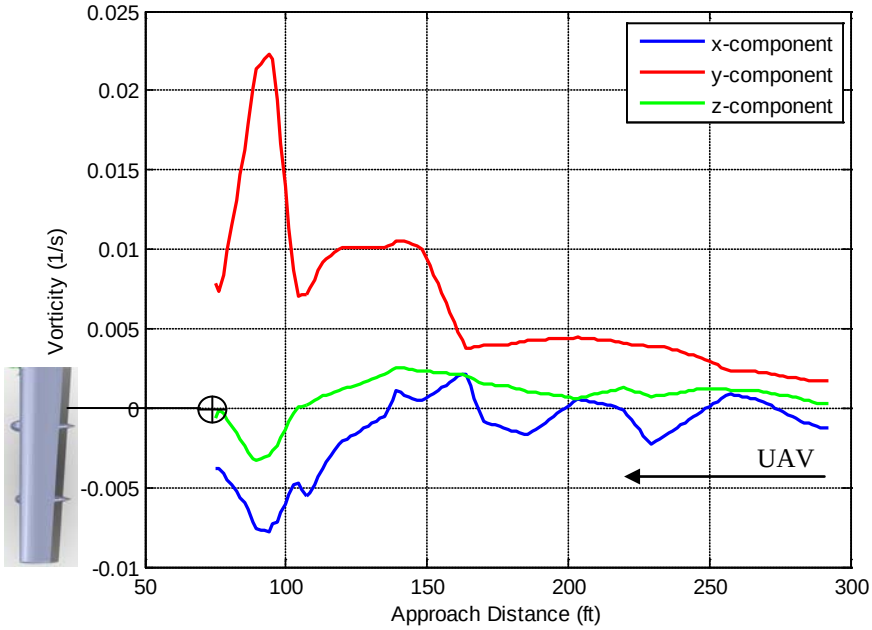

Figure 3.8 – Vorticity Profile for Straight-On Approach

3.2 Control Systems

Tier II UAVs are typically controlled at a ground control center, with one to two pilots serving as the main controllers. Figure 3.9 provides a representation of this setup. This is not necessarily an image of a ground control station for Tier II UAVs, but gives an idea as to what one might look like.

Figure 3.9 – Representative UAV Ground Control Center

The pilot may be hundreds or thousands of miles away from the UAV and cannot physically sense what the UAV may "feel" as a pilot would. This constraint limits the pilot to where he can fly the UAV. For example, flying into the vortex shed from a C-130, as discussed in Section 3.1, could be very difficult for a ground control pilot to perform. Providing the pilot the ability to essentially "flip a switch" to initiate terminal guidance for UAV-AAR would ease the control load for aerial refueling. However, the pilot would need to know the best time in which to initiate the system – knowing the terminal flight arena for which the UAV can no longer be flown by the pilot. As will be described in the following subsection, the terminal flight arena will be largely defined by changes in the flow-field which the UAV is flying. At a specified distance from the drogue, the pilot will be able to initiate the "hands-free" terminal guidance control for the remainder of the UAV-AAR docking process.

3.3 Terminal Flight Arena Definition

A UAV's pilot is constrained to a small room, not enabling him to quickly respond to rapid changes in the airspace in which the UAV is flying. In the case of UAV-AAR, the UAV will be flying in a highly active flow-field, as has been shown and described in Section 3.1. To properly define the terminal arena in which the pilot will no longer be able to control the aircraft without the aid of an autonomous system utilizing trajectory generation and regulation capability through sensor fusion and task allocation, the velocity and pressure profiles of the flow-field behind the tanker wing were used. Figure 3.10 shows a further representation of the pressure-field of the flow as it continues past the wing of the tanker.

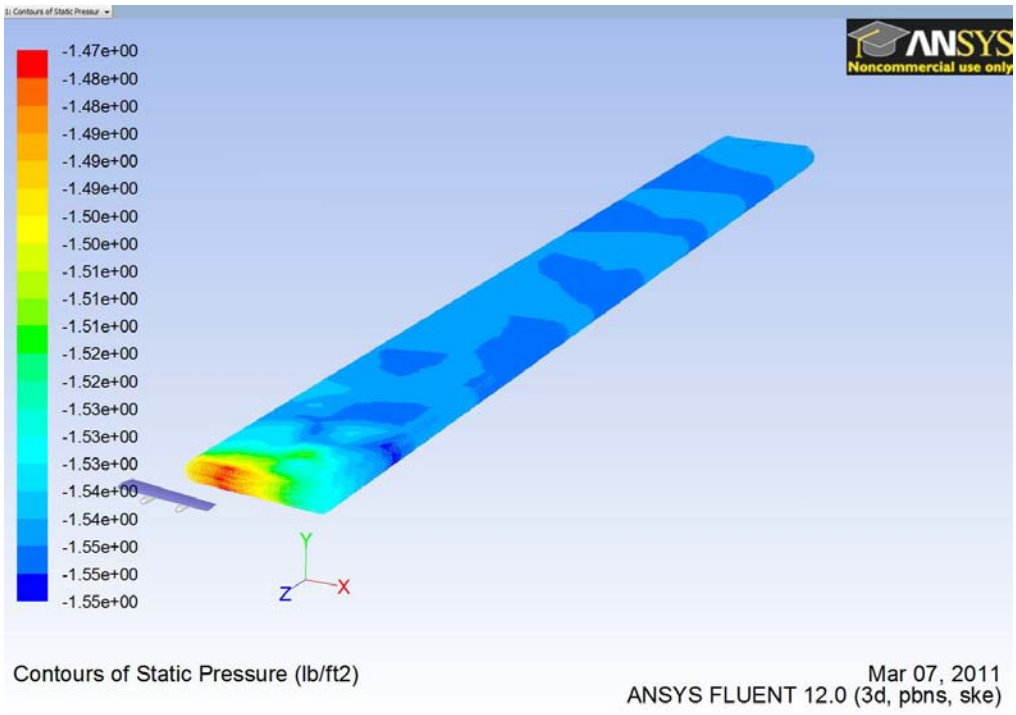

Figure 3.10 – Pressure Contours with Vortex Visualization

The vortex propagation can be visualized in Figure 3.10, which further shows the importance of determining the terminal flight arena. As aforementioned, according to Figure 3.6 and Figure 3.8, the terminal flight arena should begin around 250 feet directly behind the wing. This location is where pressure, vorticity, and velocity begin to change substantially. These changing parameters cause higher rates of perturbed flow and external forces begin acting on the UAV, which will be further discussed in Chapter 4. This will define the distance from UAV-AAR initiation to a rendezvous at the drogue to be about 175 feet. Figure 3.11 provides a demonstration, using Figure 3.1, of the terminal flight arena definition.

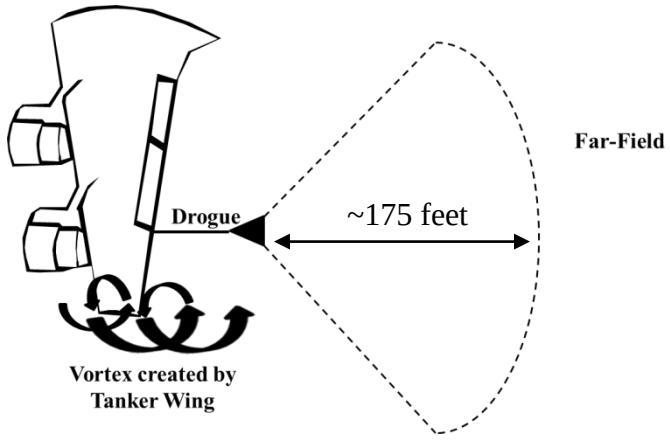

Figure 3.11 – Terminal Flight Arena Definition

CHAPTER 4

UAV FLIGHT PATTERNS

4.1 Terminal Guidance System Transition

When performing aerial refueling, there may become a point at which the UAV's pilot can no longer control the UAV effectively from the ground control center. When entering the wake of a tanker, or the terminal flight arena, a ground control pilot might have a limited ability to fly. Switching to an adaptable autonomous system at this point would enable the UAV to transmit and receive signals to determine the drogue's location with respect to its own and determine the quickest path to dock with the drogue. To account for the possibilities of different locations to initiate transition, multiple fixed-flight patterns, within the terminal flight arena, were analyzed in order to better help the development of terminal guidance for UAV-ARR.

4.2 Fixed-Flight Patterns

To assist in the development of the terminal guidance system, fixed aerial refueling flight patterns were analyzed in conjunction with the aerodynamic effects from the tanker's wake. These patterns provide insight into determining the best possible approaches to and potentially within the terminal flight arena when performing UAV-

AAR. This was completed by calculating the changing forces that the UAV would encounter as a result of the tanker wake. The induced angle of attack, or the resultant change in the longitudinal direction (Figure 4.1), the induced sideslip angle, the resultant change in the lateral direction (Figure 4.2), and the induced rolling moment (Figure 4.3) were calculated to help determine what controls would be necessary for these flight paths.

Figure 4.1 – Angle of Attack

In Figure 4.1, α denotes the angle of attack, which is the angle that is changing the pitch angle of the aircraft. In the following subsections, it will be shown how this induced angle of attack changes as the aircraft approaches the location of the drogue.

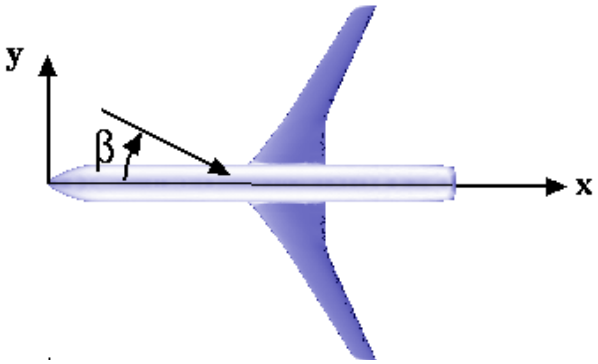

Figure 4.2 – Sideslip Angle

Figure 4.2 above shows the induced sideslip angle, denoted as β. This angle changes the yaw and roll angle of the aircraft, requiring the UAV to counter the induced angle to maintain steady flight.

Figure 4.3 – Rolling Moment

Figure 4.3 shows the induced rolling moment of the aircraft. The sideslip and rolling moment of the aircraft is coupled; but for simplification purposes, these induced forces will be uncoupled. This simplification is worthwhile to further understanding the nature of the UAV-AAR, but may not be realistic for real-world applications.

4.2.1 Flight Path Definitions

There were various fixed-flight path definitions that were selected for analysis. Each pattern selected was fixed, as a "straight-path" approach. Flight paths began either as a direct approach straight behind the drogue, or an approach coming from five and ten degrees above and below, from 45 degrees to the side, and a 45 degree diagonal approach. This was done to encompass the full area that defines the terminal flight arena.

Figure 4.4 displays a straight-on fixed flight path definition; one of the approaches used in this portion of the analysis.

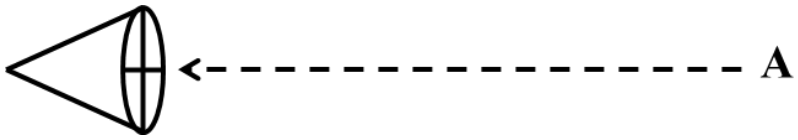

Figure 4.4 – Straight-on Approach

The cone shaped figure represents the side-view of the drogue, and the dashed line represents the flight path which the UAV will follow for UAV-AAR.

4.2.2 Straight-On Approach

The straight-on approach corresponds with approach A in Figure 4.4. In addition, Figure 3.6 gives the velocity profile for a straight-on approach with respect to distance from the drogue. The induced angle of attack was determined using a geometric method relating the velocity components in both the x- and z-direction. These velocities were exported from CFD analysis as data points up to and within the terminal flight arena, ranging from about 75-300 feet away from the tanker wing. Note that this analysis for the straight-on approach, as well as the other approaches, is a quasi-steady analysis; time is not a factor for determining induced forces and required control deflections. Figure 4.5 shows the induced angle of attack changes with respect to approach distance for the direction of flight for a straight-on approach flight pattern.

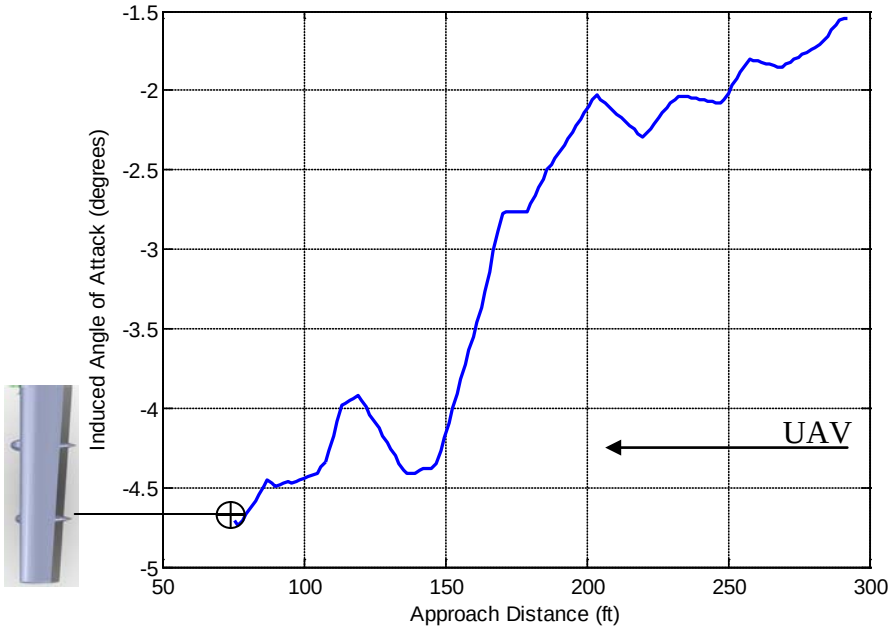

Figure 4.5 – Induced Angle of Attack: Straight-On Approach

This plot shows how the induced angle of attack changes as the UAV approaches the drogue; the image overlaying the plot shows where the UAV begins its flight in the terminal arena, and shows the location of the drogue. The maximum angle of attack being induced on the UAV is about -4.75 degrees, forcing the UAV to pitch down if uncontrolled. However, in order to maintain steady flight, on this fixed flight-path, the UAV must use the longitudinal control surfaces to counter the pitching moment that is occurring due to this induced angle of attack. In conventional aircraft, these control surfaces are called elevators; however, for the UAV that is representative of the MQ-9, the control surfaces are located on a V-tail, causing the control surfaces to act as both a rudder and elevators. For simplification, these control surfaces have been decoupled for the purpose of this study. To determine the required control surface deflection for steady

flight through the terminal flight arena, the following method[11] was used for the decoupled case:

$$\begin{bmatrix} C_{m_{\delta e}} & 0 & 0 \\ 0 & C_{n_{\delta R}} & 0 \\ 0 & 0 & C_{l_{\delta A}} \end{bmatrix} \begin{bmatrix} \delta e \\ \delta R \\ \delta A \end{bmatrix} = \begin{bmatrix} -C_{m_0} + C_{m_\alpha}\alpha \\ -C_{n_\beta}\beta \\ C_l + C_{l_\beta}\beta \end{bmatrix}$$

A plot of elevator deflection with respect to distance from the drogue is shown in Figure 4.6. This plot is similar to Figure 4.5, in that it follows the same trend.

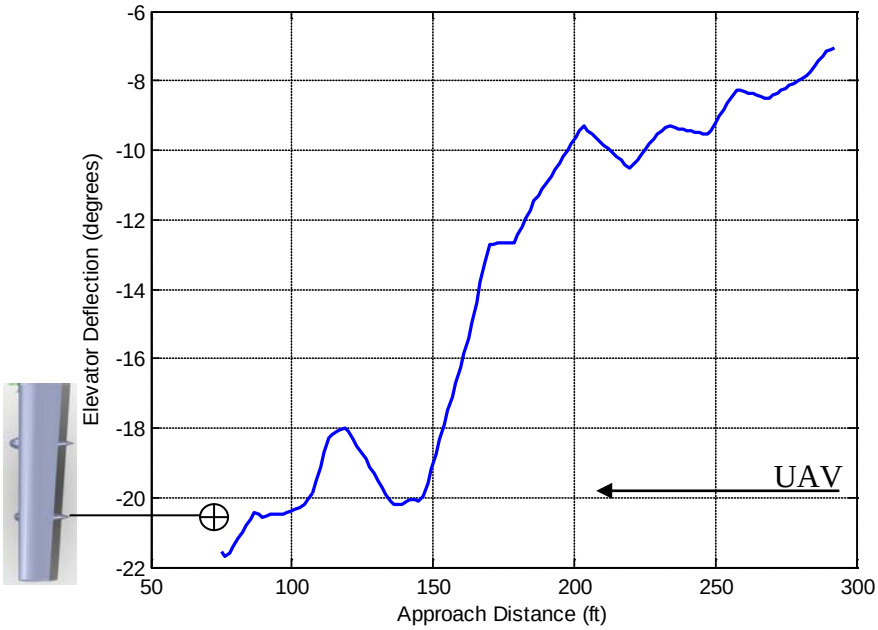

Figure 4.6 – Required Elevator Deflection: Straight-On Approach

As displayed, the maximum elevator deflection angle needed to counter the maximum induced angle of attack is around -22 degrees. This is necessary for maintaining longitudinal steady flight while traveling in the wake of the tanker.

Concerning lateral and directional control, the induced sideslip angle was calculated using a geometric method relating the velocity component in the x- and y-directions. These velocities were found in the same way as before using CFD by taking data points up to and within the terminal flight arena, ranging from about 75-300 feet away from the tanker wing. Figure 4.7 shows a plot of induced sideslip angle with distance to the drogue for the straight-on approach, similar to that of Figure 4.4.

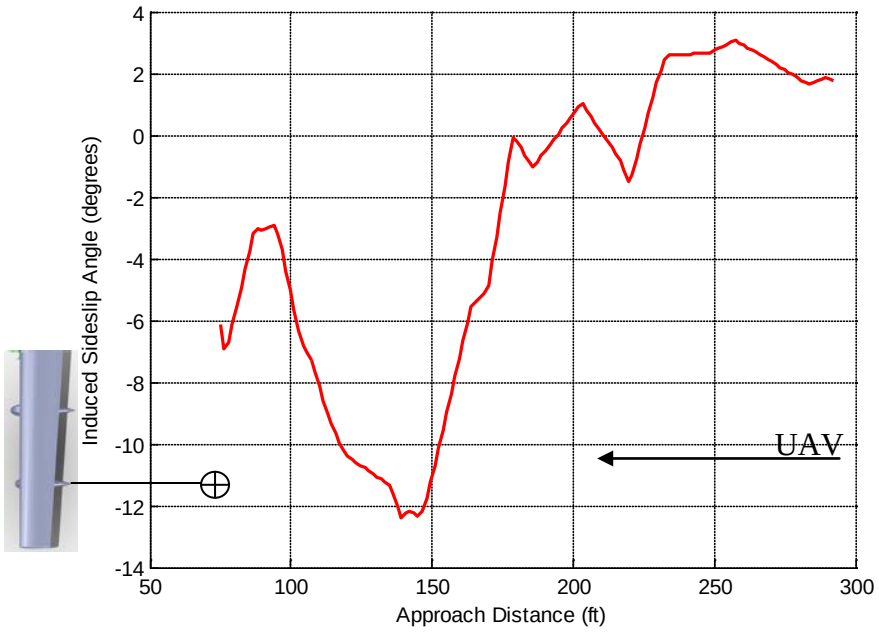

Figure 4.7 – Induced Sideslip Angle: Straight-On Approach

This plot shows that the maximum induced sideslip angle acting on the UAV is about -12.5 degrees. The lateral control surface of the UAV is called a rudder, and the change in its deflection angle throughout the straight-on approach is plotted in Figure 4.8.

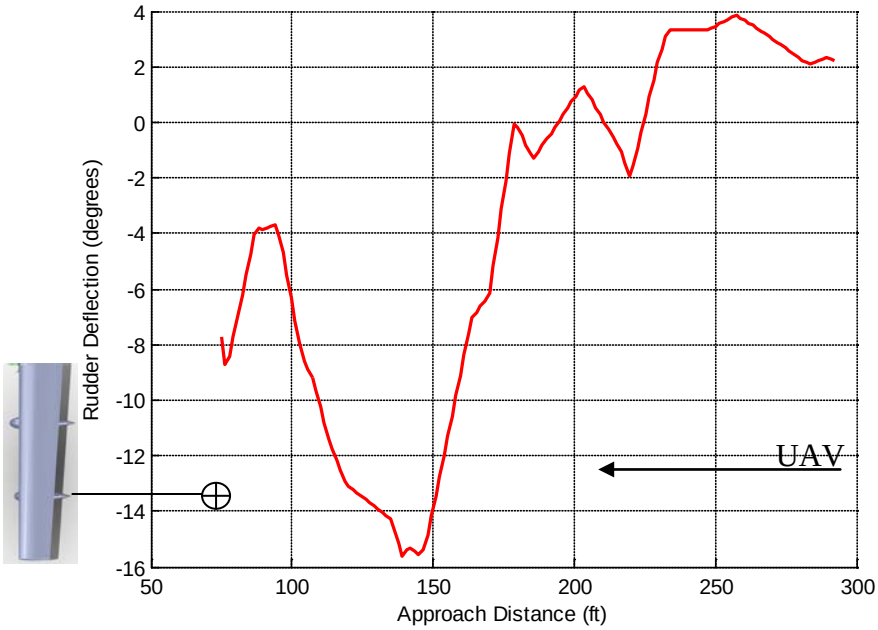

Figure 4.8 – Rudder Deflection: Straight-On Approach

According to Figure 4.8, the maximum rudder deflection will be about -15 degrees. In addition to sideslip angle and rudder deflection, there will be an adverse roll induced on the UAV while in the terminal flight arena. Figure 4.9 shows a plot of induced roll with respect to approach distance just as Figures 4.5 and 4.7 are plotted.

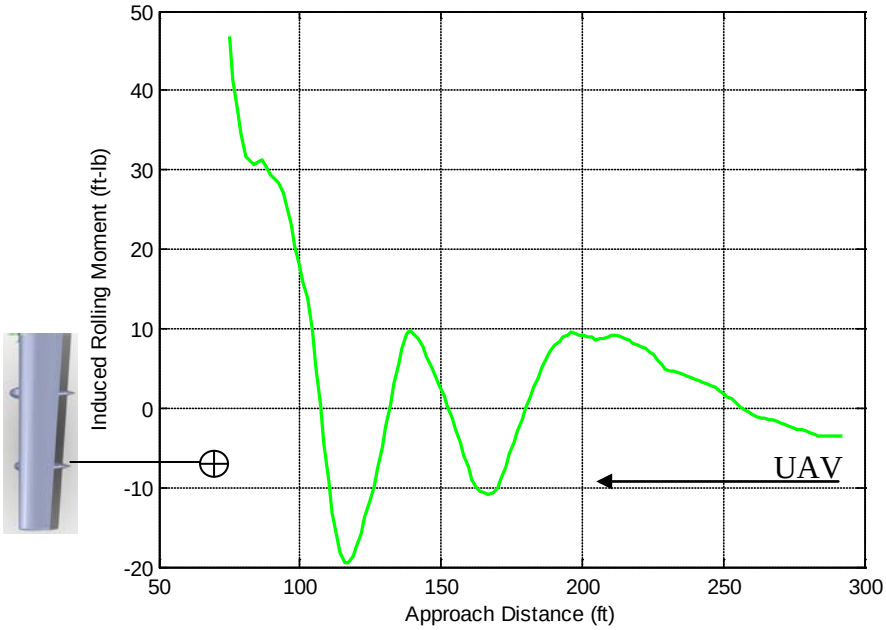

Figure 4.9 – Induced Rolling Moment: Straight-On Approach

The induced rolling moment was calculated by finding the pressure gradient across the span of each wing of the UAV and placing the mean value of the gradient from each wing at its midsection and calculating the force across the wing area, and then calculating the moment. These rolling moments are corrected by using control surfaces called ailerons. A plot of aileron deflection with respect to approach distance is shown in Figure 4.10. Note that the maximum aileron deflection is about -2.5 degrees.

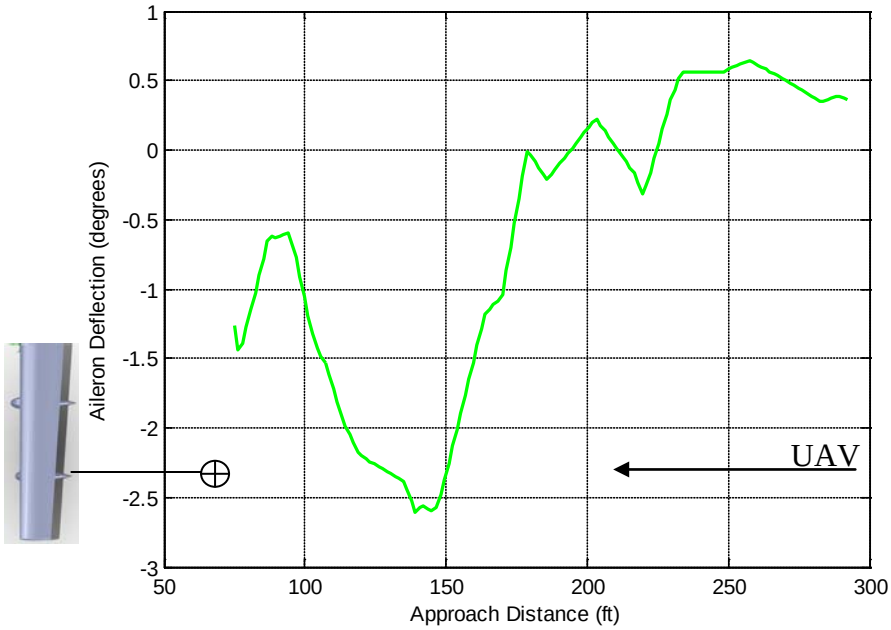

Figure 4.10 – Aileron Deflection: Straight-On Approach

The above analysis was completed for a straight-on approach; there are many other approaches that may prove beneficial when approaching and flying within the terminal flight arena, a few of which are presented in the following subsection.

4.2.3 Approaches

There are multiple approach angles and directions at which the UAV can take in order to successfully dock to the drogue. These approaches include, but are not limited to, an above and below approach, a side approach, and a diagonal approach. The first to be discussed is a below approach. This analysis was similar to that of the straight-on approach, but the flight path was set to be at an angle of five and ten degrees below the straight-on approach, labeled as path B and C, respectively, in Figure 4.11.

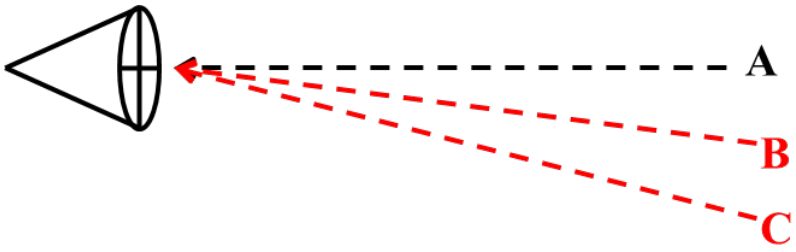

Figure 4.11 – Below Approaches

The induced angle of attack and induced sideslip angles were calculated using the same methods as described in the previous section. The data points were taken from CFD in lines similar to that shown in Figure 4.11. These changes in induced forces and induced rolling moment are represented in Figures 4.12 through 4.15, each in variation with respect to distance from the drogue's location.

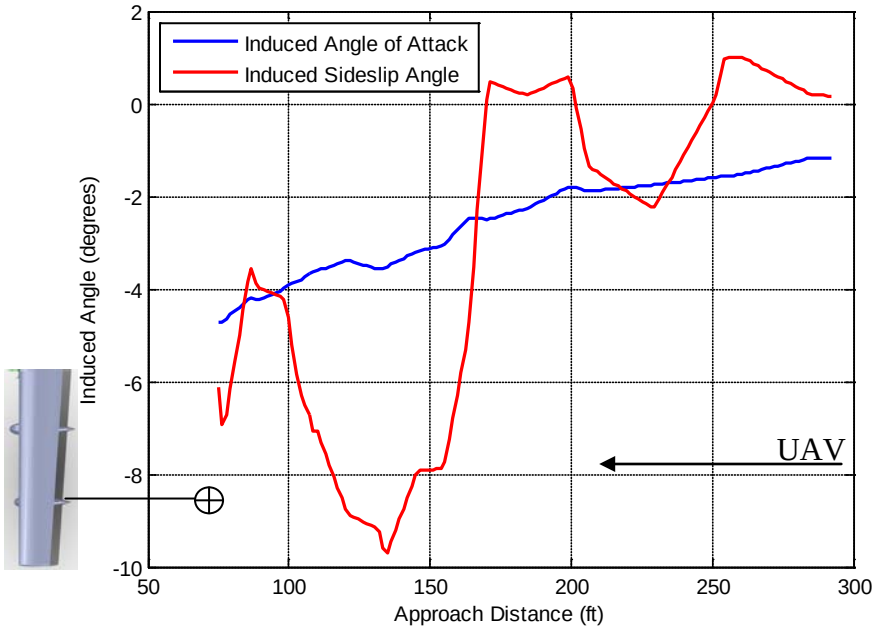

Figure 4.12 – UAV-AAR Induced Forces: 5 Degrees Below Approach

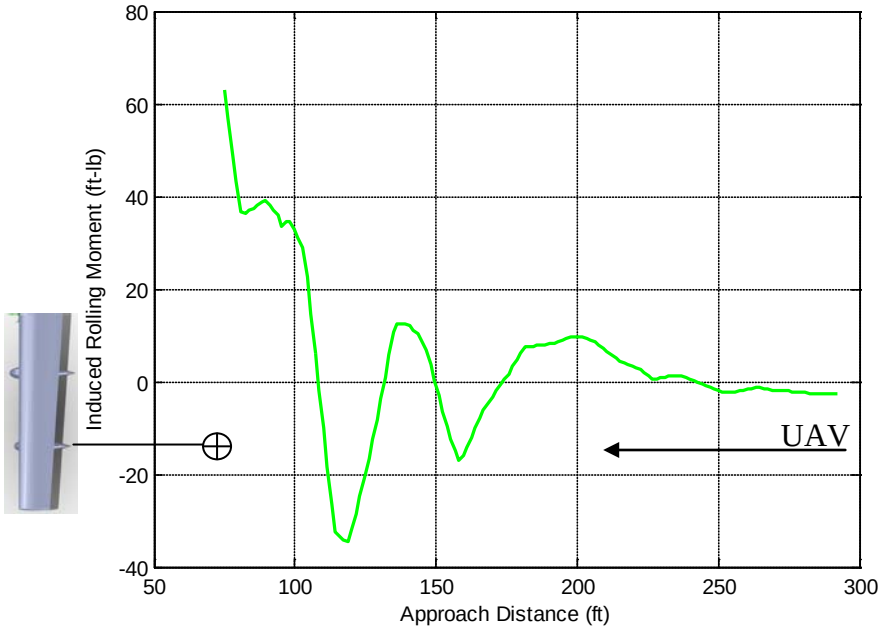

Figure 4.13 – UAV-AAR Induced Rolling Moment: 5 Degrees Below Approach

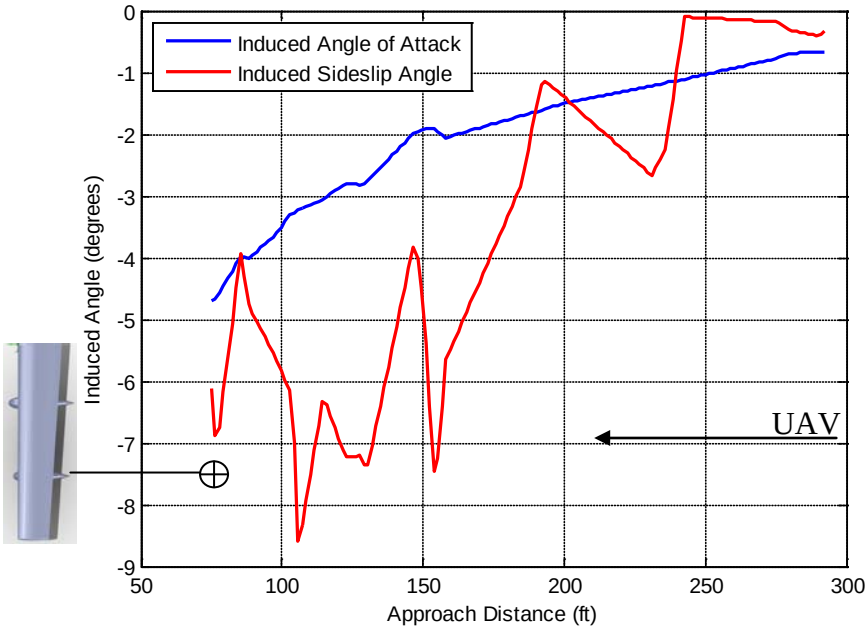

Figure 4.14 – UAV-AAR Induced Forces: 10 Degrees Below Approach

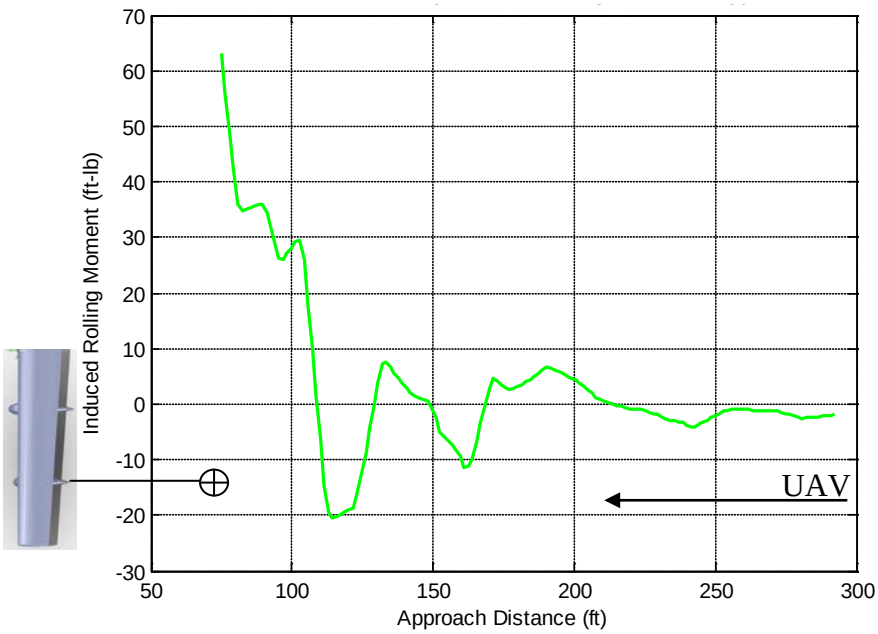

Figure 4.15 – UAV-AAR Induced Rolling Moment: 10 Degrees Below Approach

Figures 4.12 through 4.15 can be compared with Figures 4.5, 4.7, and 4.9 to view how the induced forces acting on the UAV change as the approach angle decreases. Figures 4.16 and 4.17 show the respective control surface deflection changes for the below approaches.

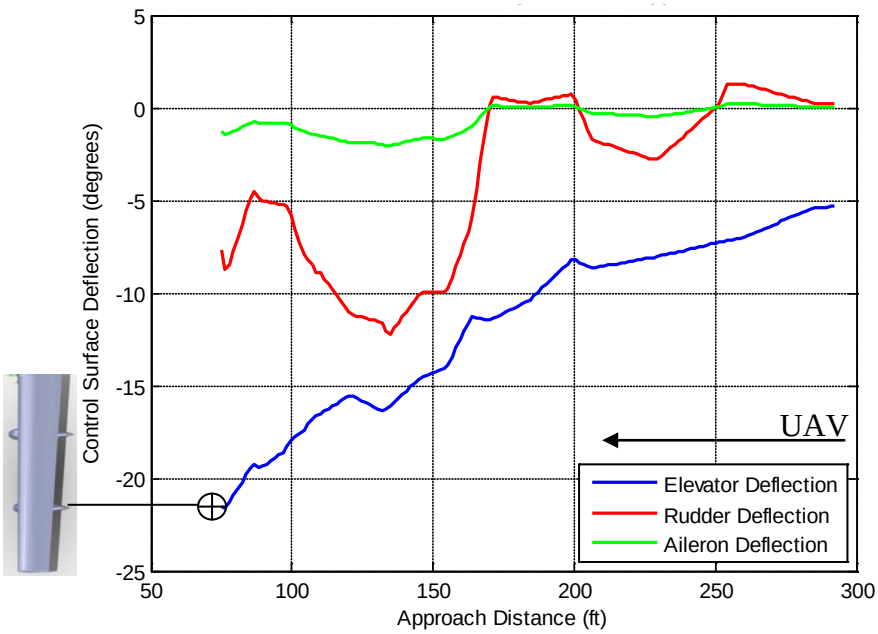

Figure 4.16 – UAV-AAR Controls: 5 Degrees Below Approach

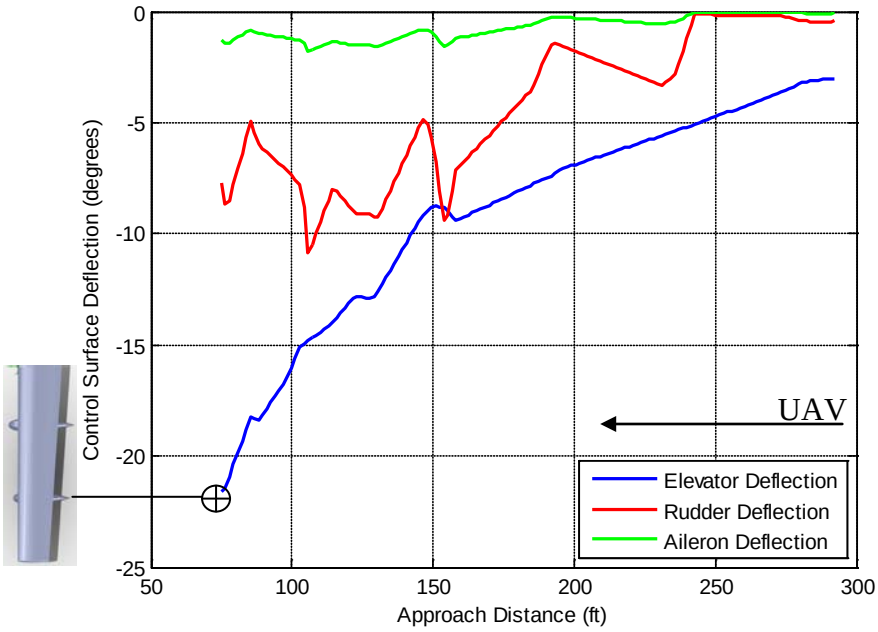

Figure 4.17 – UAV-AAR Controls: 10 Degrees Below Approach

These plots show that the maximum elevator deflection angle (-22.5 degrees) is the same for all flight paths, due to the fact that this force is occurring at the drogue's location. It can be seen that the below approaches reduces the maximum sideslip and rudder deflection angle, required for stable flight in the terminal flight arena. As a matter of fact, the overall range of deflection is reduced the most in the ten-degrees-below approach.

The next set of approaches to be discussed are the above approaches, seen in Figure 4.18. The drogue is still displayed as in Figure 4.11, but now the approach angles increase to 5 and 10 degrees above the straight-on approach, labeled as approaches D and E, respectively.

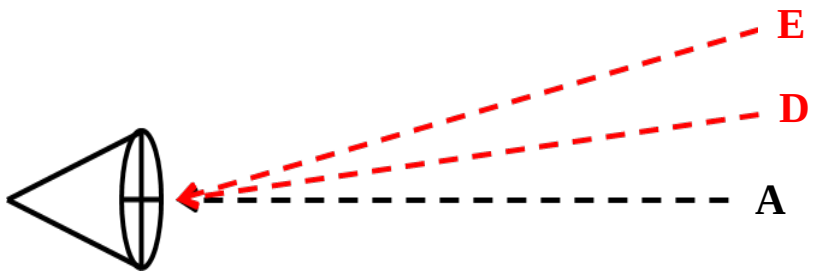

Figure 4.18 – Above Approaches

All induced force and induced rolling moment plots for this set of approaches can be found in Appendix A, Figures A.1 to A.4. To understand the behavior of the control surfaces for the above approaches, Figures 4.19 and 4.20 plot the control surface deflections as the UAV approaches the drogue.

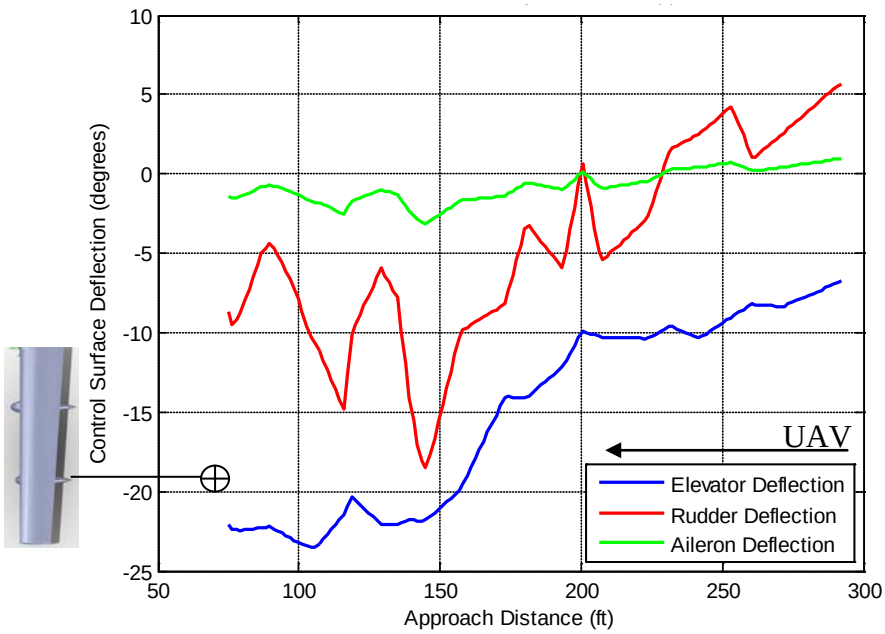

Figure 4.19 – UAV-AAR Controls: 5 Degrees Above Approach

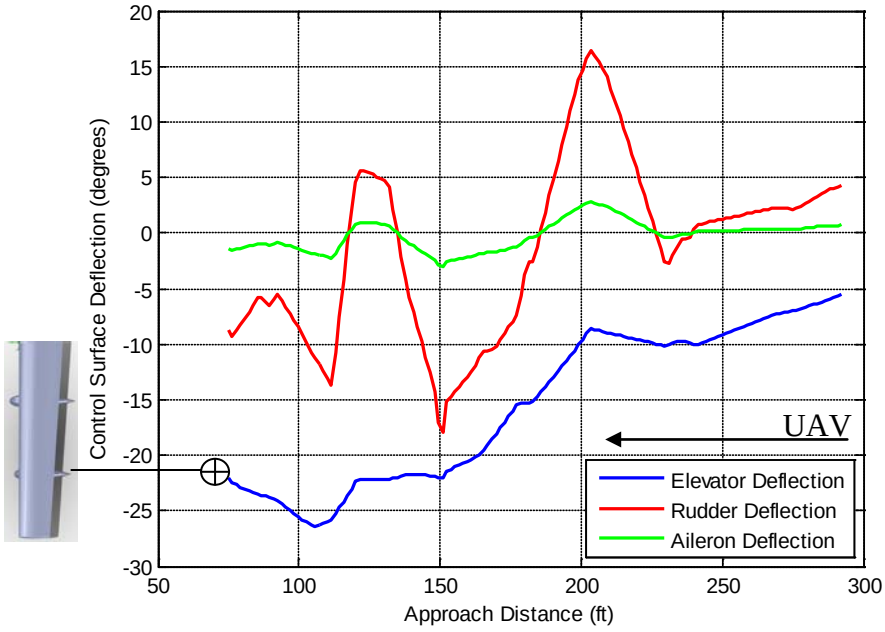

Figure 4.20 – UAV-AAR Controls: 10 Degrees Above Approach

In contrast to the below approaches, the control surface deflections for both the elevator and rudder increase as the approach angle increases above the straight-on approach.

The next approach to be discussed is the side approach, seen in Figure 4.21. The drogue is now displayed in a top-down view so that the side approach (labeled as F) can be easily visualized. The flight path is designed so that the UAV will approach at an angle of 45 degrees from the straight-on path, labeled as A in the figure.

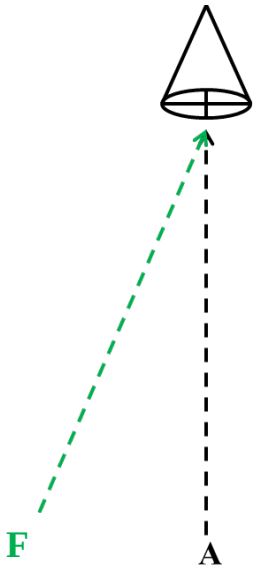

Figure 4.21 – Side Approach

With the side approach, the UAV will not be flying directly in the path of the tanker wing's vortex, but will meet with it a later point in the terminal flight arena. Figure 4.22 provides a plot of these changes in control surface deflection for a side approach. Figures A.5 and A.6 in the appendix are plots of the induced forces and induced rolling moment for a side approach.

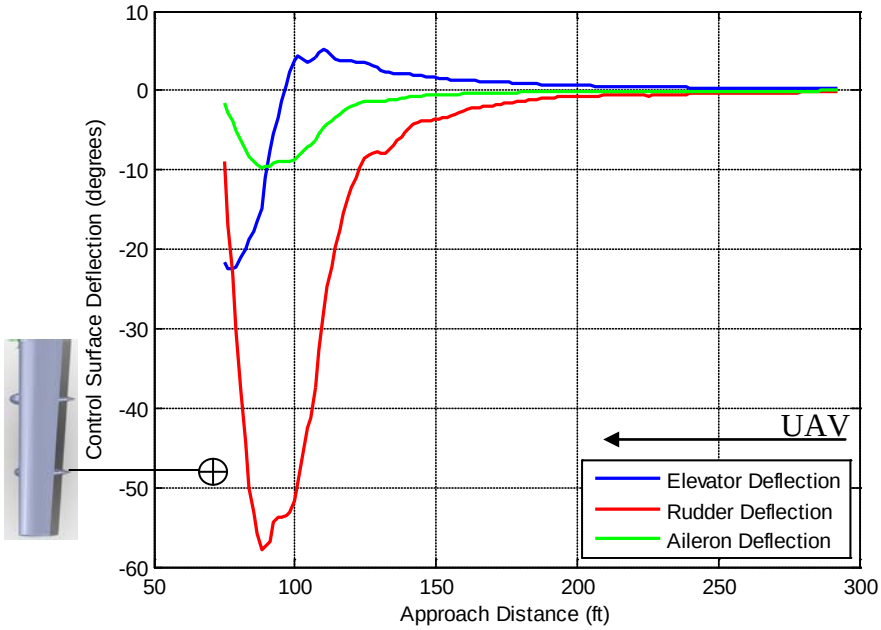

Figure 4.22 – UAV-AAR Controls: Side Approach

The induced angles of attack, and therefore the elevator deflection angles, are much different than those shown in Figures 4.5 and 4.6. With this figure, the location at which the UAV enters the vortex can be visualized, and is located at around 120 feet from the tanker's wing. This is where the spike in rudder deflection occurs, and then immediately drops as it approaches the drogue. According to this plot, the maximum rudder deflection angle is around -57 degrees, a drastic change in comparison to what is shown in Figure 4.8. Again, this plot displays where the UAV would enter the vortex – the negative spike in the data denotes this location.

The final approach to be discussed is the diagonal approach from both below and above the drogue. It follows that of the side approach, but begins at a location 45 degrees below and above. This can be seen in Figure 4.23 with the diagonal approach labeled as G for the below approach and H for the above approach. The straight-on approach can

no longer be seen due to the orientation of the image, as it is directly in line with the drogue.

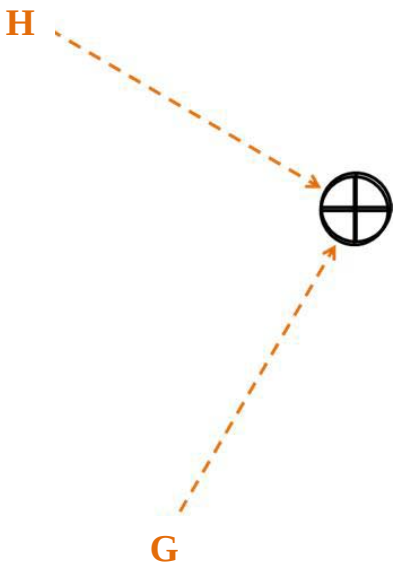

Figure 4.23 – Diagonal Approach

This flight path seems to reduce the impact of the vortex on the UAV as it approaches the drogue. Figures 4.24 and 4.25 show the required control deflection plots with respect to distance from the drogue's location. Figures A.7 through A.10 display plots of induced forces and induced moment for the below and above diagonal approaches.

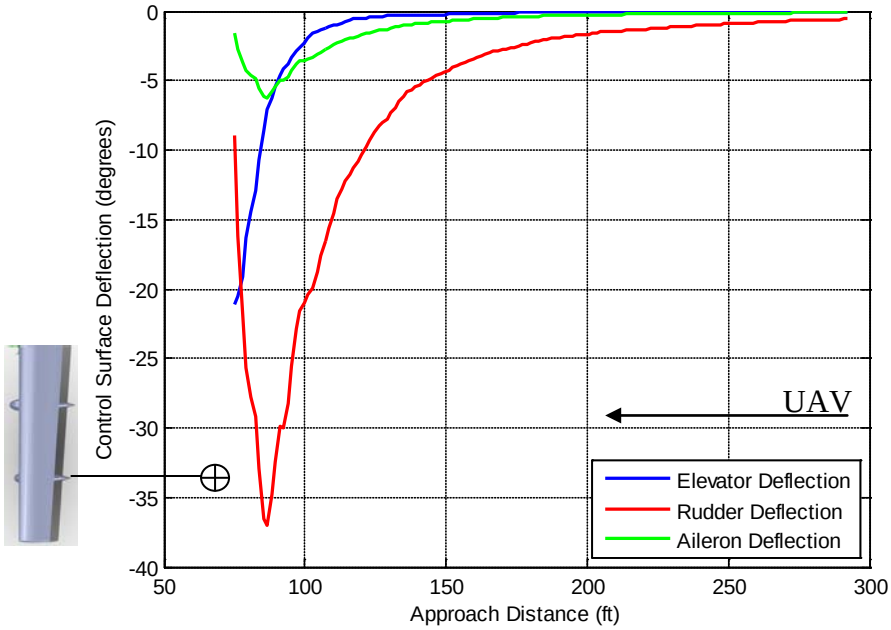

Figure 4.24 – UAV-AAR Controls: Diagonal Below Approach

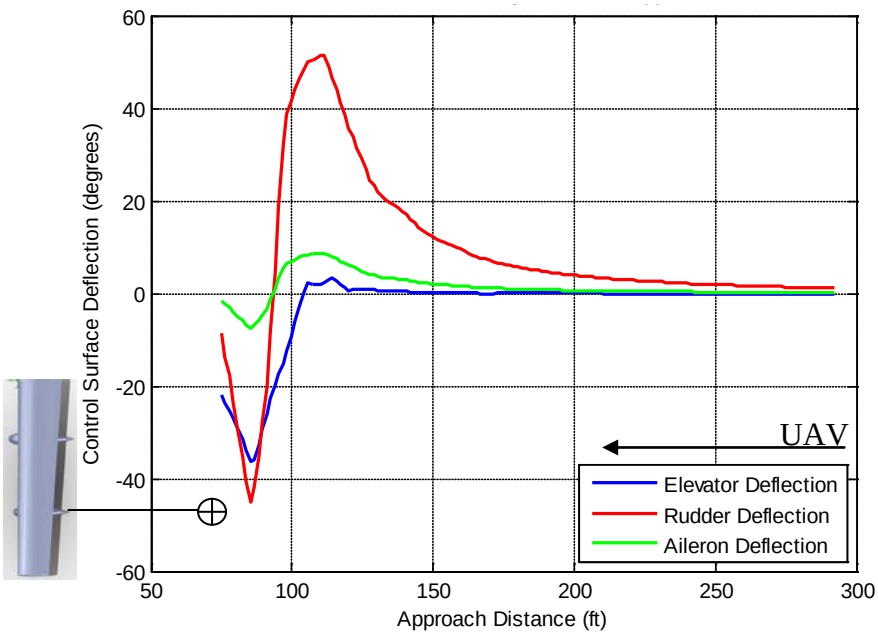

Figure 4.25 – UAV-AAR Controls: Diagonal Above Approach

In addition, rudder deflection reduces during a diagonal flight pattern, in comparison to the side approach. A problem that can be foreseen with these charts is the fact that the

rudder will be changing deflection quite extensively throughout flight, for both the above and below approaches. This is due to the way in which the UAV enters the tanker's wing vortex.

The purpose for determining these fixed-flight patterns and analyzing the required control surface deflections for the terminal flight arena was to use them to assist in developing a strategy for an autonomous system. The goal is that the system will extrapolate the data to find all forces in the terminal flight arena. The following section will discuss the autonomous implementation.

4.3 D-O.P-P. Implementation

The Dual-Optimal Path-Planning (D-O.P-P.) technique[1] will be used for autonomous implementation. This technique, in general form is defined by the following figure:

Driver:

Minimize $f(\mathbf{x})$; *subject to* $g_i(\mathbf{x})$, $(i = 1,\ldots, n)$,
with solution:

$\mathbf{x}^*_k$, $(k = 1,\ldots, N)$

Path:

Minimize $J(u) = \int_0^T f_0(\mathbf{x}(t),u(t))\, dt$,
where

$\mathbf{x}(t)$, $(\mathbf{x}^*_{k-1}(t),\ldots, \mathbf{x}^*_k(t))$: $[0,T] \rightarrow R^n$
is the solution of the differential system with boundary conditions
and with initial and final conditions

$d\mathbf{x}_j/dt = f_j(\mathbf{x}, u(t))$, $(j = 1,\ldots, n)$;
$\mathbf{x}(0) = \mathbf{x}^*_{k-1}$; $\mathbf{x}(T) = \mathbf{x}^*_k$
where

$J(u^*) = \min J(u)$
with u^* and the associated path $\mathbf{x}$ called 'optimal.'

Figure 4.26 – D-O.P-P. Technique

This technique will use trajectory generation and regulation capability through sensor fusion and task allocation in close proximity to obtain docking with the drogue. The D-O.P-P. technique is proven and will be useful for developing the autonomous system and future control laws.

4.3.1 Methodology

In order to determine how the D-O.P-P. technique will work, a cycle was developed. Figure 4.27 is a representation of this cycle.

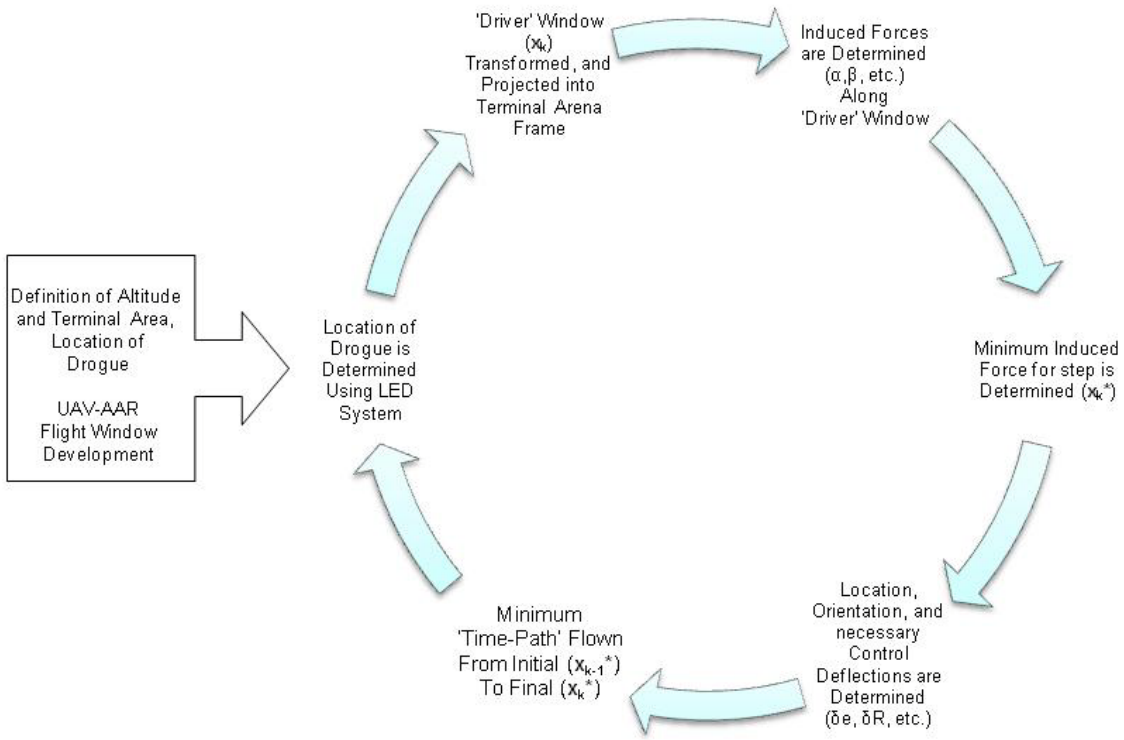

Figure 4.27 – D-O.P-P. Flowchart for UAV-AAR

As shown, the technique will first establish the altitude and terminal flight arena definition in proximity to the UAV, and will also determine the location of the drogue. This will allow for UAV-AAR flight window development, which will be determined based on the UAVs maximum performance maneuvers. This driver window will then be transformed and projected into the terminal flight arena frame. Once the window has been transformed, the location of the drogue is determined using sensor fusion – hardware and methods available were discussed in Section 2.4. Next, the induced forces are determined along the drive window, and the minimum induced force for the step will be determined. The location, orientation, and necessary control deflections are then determined for this location $\mathbf{x}^*_k$. Finally, the minimum "time-path" is flown from the UAV's initial location to its next destination in the step. Then the process is repeated. The goal behind this methodology is to reach the drogue as quickly as possible without performing extraneous maneuvers and control deflection by flying a minimum induced force approach on the way through the terminal flight arena.

CHAPTER 5

CONCLUSION

UAVs will be expected to remain in flight for long periods of time; one major constraint is the fact that the range of UAV is limited to its fuel capacity. Terminal guidance for UAV-AAR using a probe-and-drogue refueling configuration is a method that could be used for aerial refueling of UAVs. In order to begin development of terminal guidance, the terminal flight arena for which the system will be initiated was determined to begin at about 175 feet from the drogue's location. A quasi-steady analysis showed that the best fixed-flight path approach would be at ten degrees below the straight-on approach, with a maximum elevator deflection of about -22 degrees, a rudder deflection of about -11 degrees, and minimal aileron deflection. This fixed-flight path approach also resulted in the most minimal change of control surface deflection throughout the terminal flight arena. The full fixed-flight path analysis can be used to assist in developing a strategy for an autonomous system. In order to develop this system, the D-O. P-P. technique will be implemented and tailored for UAV-AAR. As determined, the cycle for the autonomous system will start by defining the flight conditions and locating the drogue and its orientation through the developed LED system. The system will then proceed to transform the driver window, defined by the UAV's

mechanics and performance parameters, and project it into the terminal flight arena. The system will continue to determine induced forces, the location of the minimum induced force while determining the quickest path to the drogue. This will then allow it to calculate the necessary control surface deflections for reaching the next location, and ultimately, the drogue.

REFERENCES

1. Whitfield, C. A., “An adaptive Dual-Optimal Path-Planning Technique For Unmanned Air Vehicles with Application to Solar-Regenerative High Altitude Long Endurance Flight,” The Ohio State University, 2009.

2. Bolkcom, C., Klaus, J.D., “Air Force Aerial Refueling Methods: Flying Boom versus Hose-and-Drogue,” CRS Report for Congress, May 2005.

3. "Boom: Definition, Synonyms from Answers.com." Answers.com: Wiki Q&A Combined with Free Online Dictionary, Thesaurus, and Encyclopedias. Web. <http://www.answers.com/topic/boom>.

4. "Hose-and-drogue In-flight Refueling System - Patent 6926049." Patent Searching and Invention Patenting Information. Web. <http://www.freepatentsonline.com/6926049.html>.

5. Staff, Benzinga. "C-130-Helicopter Mishap | Benzinga.com." *Benzinga - Stock Market News, Business News, Quotes, Ideas*. Web. <http://www.benzinga.com/general/33165/c-130-helicopter-mishap>.

6. "The World's Deadliest Drone: MQ-9 REAPER." *TwistedSifter - The Best of the Visual Web, Sifted, Sorted and Summarized*. Web. <http://twistedsifter.com/2010/05/worlds-deadliest-drone-mq-9-reaper/>.

7. Tandale, M. D., Bowers, R., Valasek, J., “Trajectory Tracking Controller for Vision-Based Probe and Drogue Autonomous Aerial Refueling,” Journal of Guidance, Control, and Dynamics, Vol. 29, No. 4, July-August 2006.

8. Valasek, J., Gunnam, K., Kimmett, J., Tandale, M. D., Junkins, J. L., and Hughes, D., “Vision-Based Sensor and Navigation System for Autonomous Air Refueling,” Journal of Guidance, Control, and Dynamics, Vol. 28, No. 5, Sept.-Oct. 2005.

9. "Probe and Drogue." *World News*. Web. <http://wn.com/probe_and_drogue>.

10. Anderson, John David. *Fundamentals of Aerodynamics*. Boston: McGraw-Hill Higher Education, 2007. Print.

11. Nelson, Robert C. *Flight Stability and Automatic Control*. Boston, MA: WCB/McGraw Hill, 1998. Print.

APPENDIX: FIXED FLIGHT PATTERNS

A.1 Induced Forces for 5 Degrees Above Approach

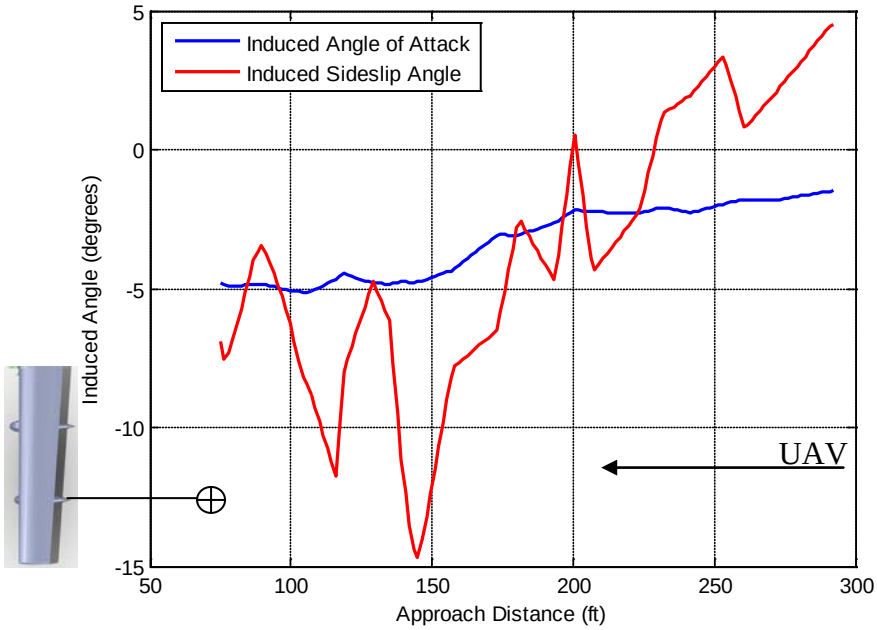

Figure A.1 – UAV-AAR Induced Forces: 5 Degrees Above Approach

A.2 Induced Rolling Moment for 5 Degrees Above Approach

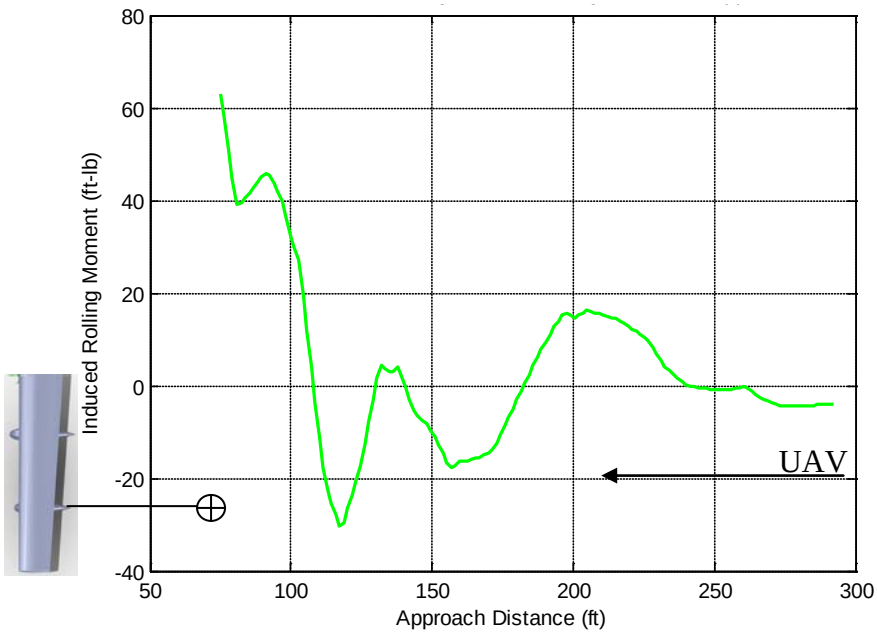

Figure A.2 – UAV-AAR Induced Rolling Moment: 5 Degrees Above Approach

A.3 Induced Forces for 10 Degrees Above Approach

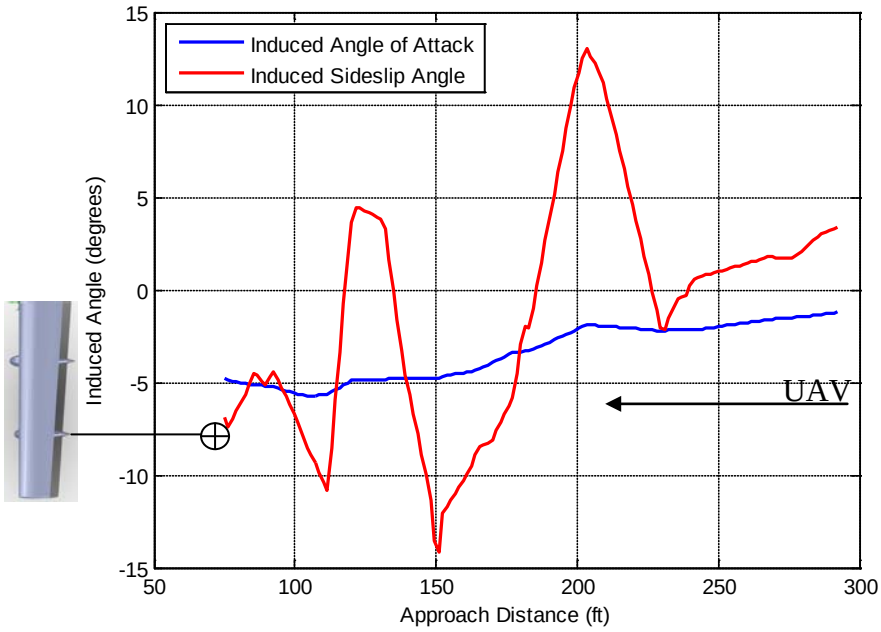

Figure A.3 – UAV-AAR Induced Forces: 10 Degrees Above Approach

A.4 Induced Rolling Moment for 10 Degrees Above Approach

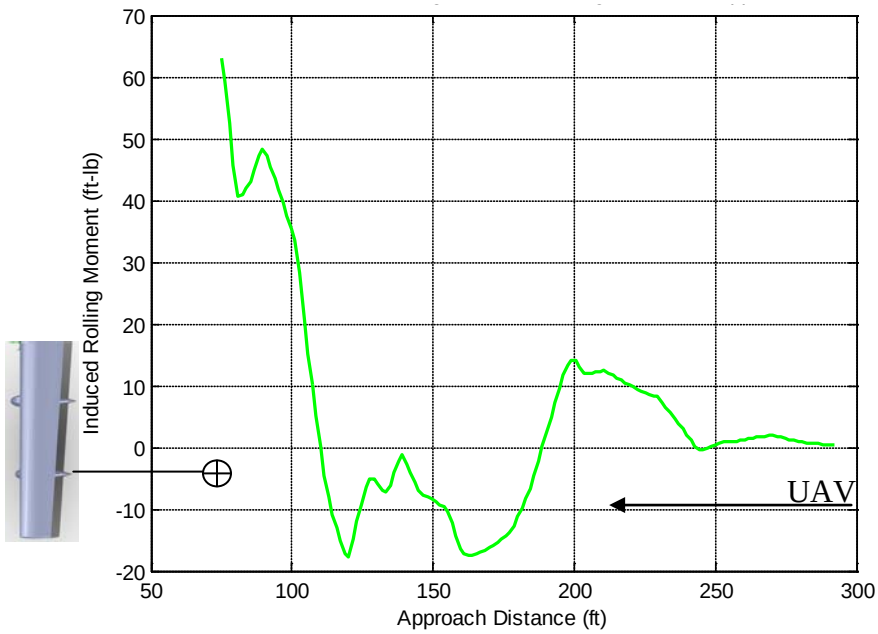

Figure A.4 – UAV-AAR Induced Rolling Moment: 10 Degrees Above Approach

A.5 Induced Forces for Side Approach

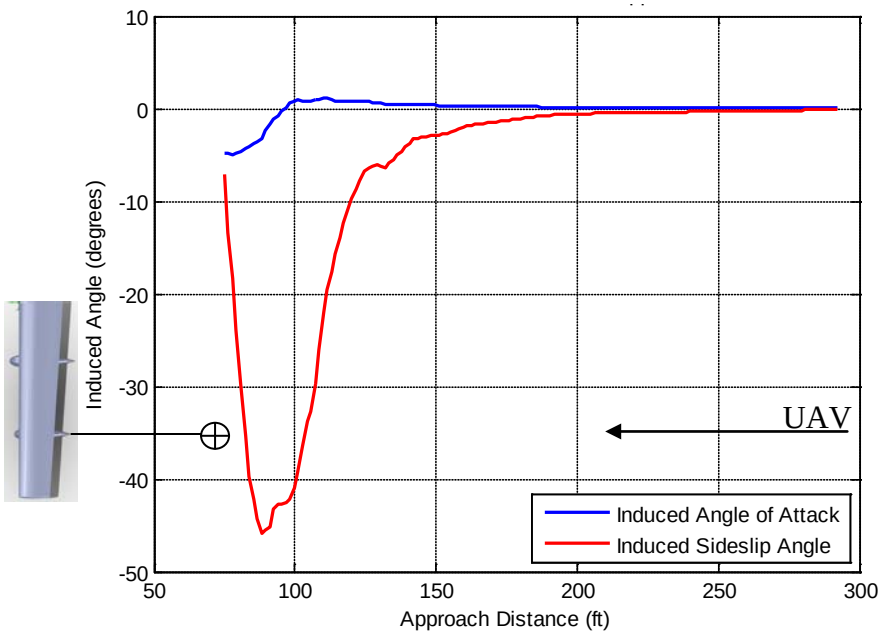

Figure A.5 – UAV-AAR Induced Forces: Side Approach

A.6 Induced Rolling Moment for Side Approach

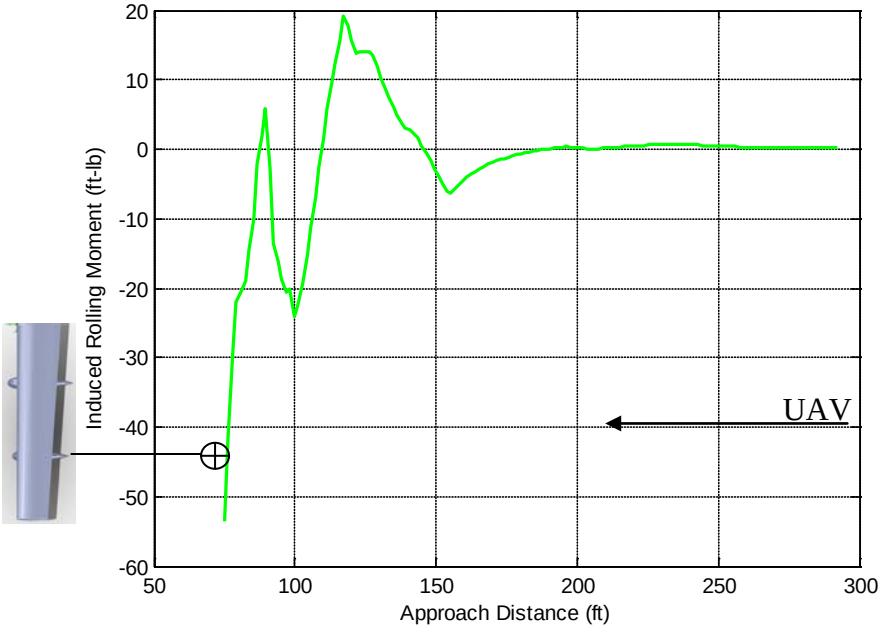

Figure A.6 – UAV-AAR Induced Rolling Moment: Side Approach

A.7 Induced Forces for Diagonal Below Approach

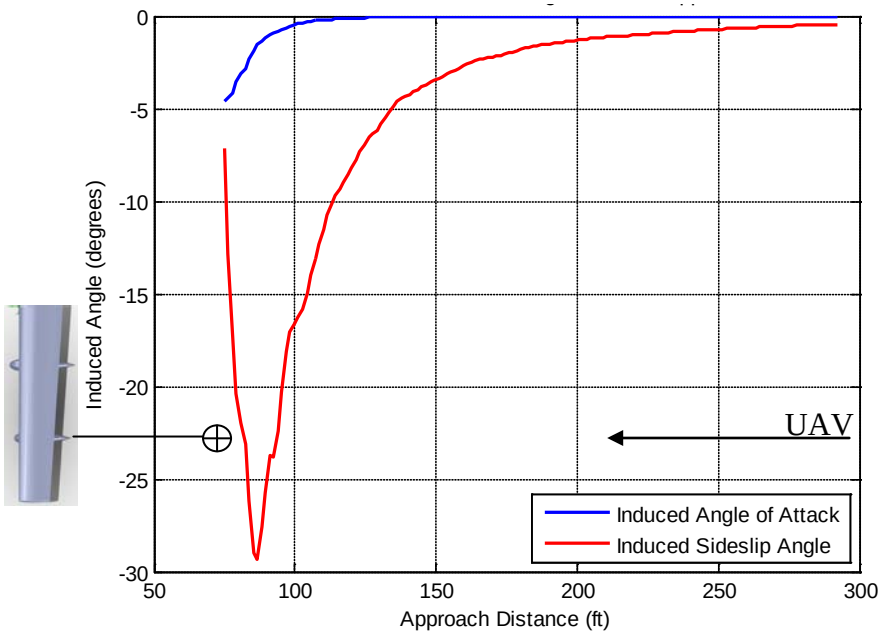

Figure A.7 – UAV-AAR Induced Forces: Diagonal Below Approach

A.8 Induced Rolling Moment for Diagonal Below Approach

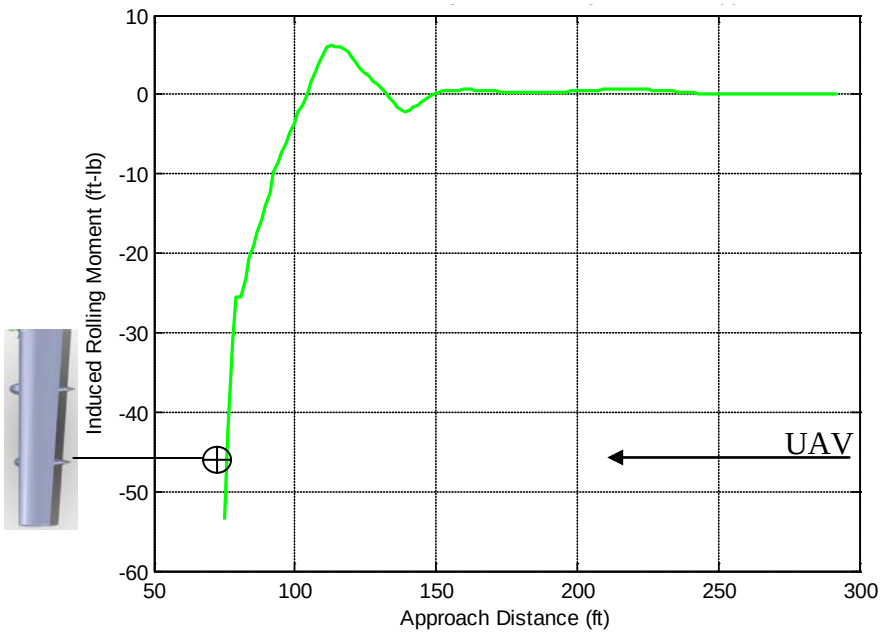

Figure A.8 – UAV-AAR Induced Rolling Moment: Diagonal Below Approach

A.9 Induced Forces for Diagonal Above Approach

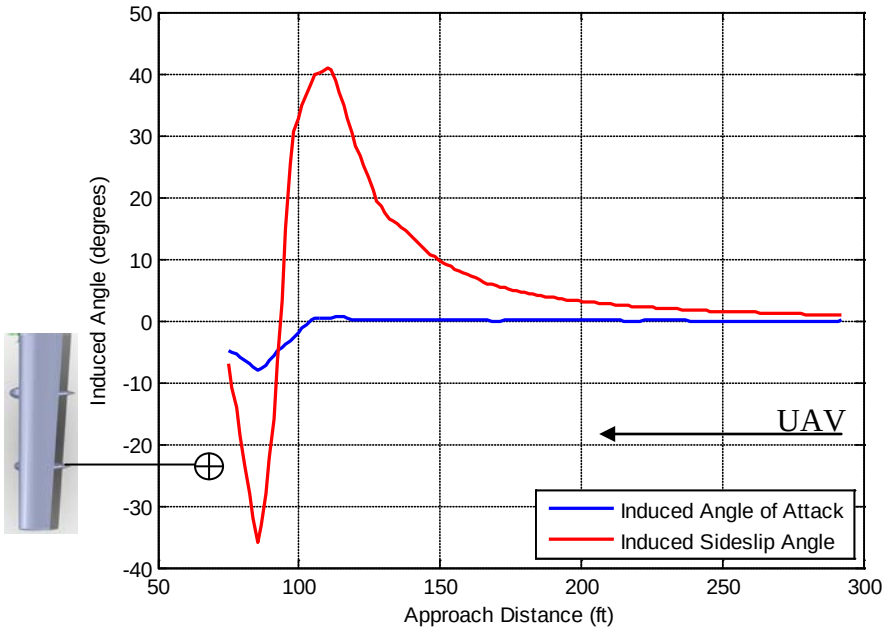

Figure A.9 – UAV-AAR Induced Forces: Diagonal Above Approach

A.10 Induced Rolling Moment for Diagonal Above Approach

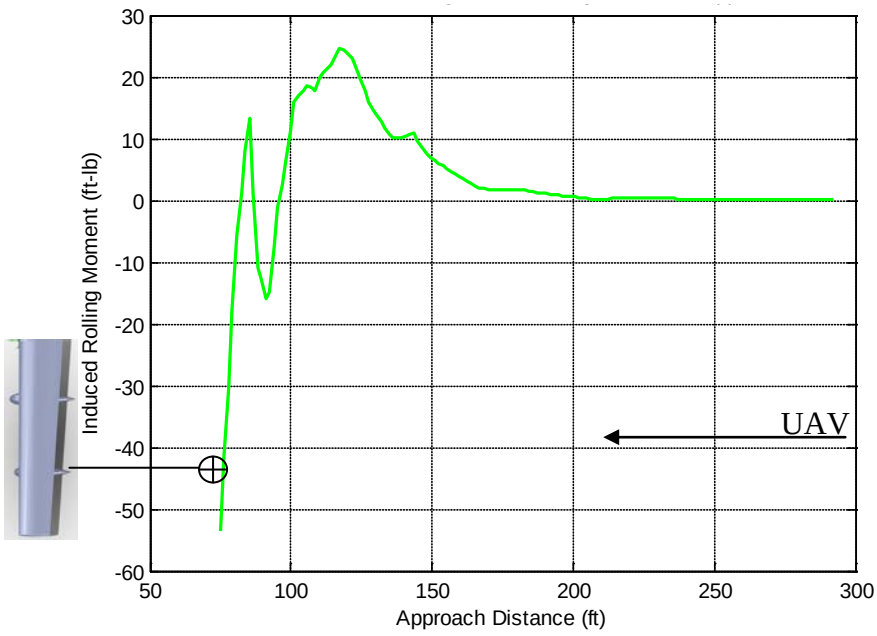

Figure A.10 – UAV-AAR Induced Rolling Moment: Diagonal Above Approach